X-616-68-345

PREPRINT

THE GEOMAGNETIC TAIL

NORMAN F. NESS

SEPTEMBER 1968

GSFC — GODDARD SPACE FLIGHT CENTER

GREENBELT, MARYLAND

THE GEOMAGNETIC TAIL

Norman F. Ness
Laboratory for Space Sciences
NASA-Goddard Space Flight Center
Greenbelt, Maryland

September 1968

Introduction

The solar wind interaction with the geomagnetic field leads to a number of distinctive and significant phenomena. The most unique of these is the formation of an extended geomagnetic tail and imbedded plasma sheet. The orientation of the field lines in the geomagnetic tail is roughly parallel or anti-parallel to the earth-sun line or equivalently the direction of solar wind flow. Approximately 5 years ago the first direct measurements of these phenomena in situ were begun systematically and since that time a great wealth of experimental evidence has been collected defining the physical properties and dynamics of the geomagnetic tail. There is as yet no agreement on the specific physical process which forms the tail. This paper summarizes the experimental observations with reference to the several theoretical models proposed (see review by Dungey, 1968). Figure 1 illustrates both the geometry of the geomagnetic tail and the earth's bow shock in cislunar space and the orbits of those satellites which have studied the geomagnetic tail.

Historial Review

Unlike the radiation belts, it cannot be said that the geomagnetic tail was unexpected theoretically. Piddington (1960), in a study of the phenomena of geomagnetic storms, suggested that the main phase decrease of the terrestrial field was associated with the formation of a magnetic tail extending from the earth on the night side. At that time, the solar wind was not considered to be a continuous flux of plasma from the sun so such a magnetic tail was thought to be only a temporary distortion of the geomagnetic field.

Subsequently Johnson (1960) considered the effect of a continuous flux of rapidly moving highly conducting solar plasma. He proposed that the principal effect would be to deform the geomagnetic field and confine it to form roughly a tear drop shape with a front to back ratio of approximately 1 to 6. He suggested that the tail field lines would not be drawn out to infinity although the possible presence of hydromagnetic waves or other energy sources might open the tail of the tear drop and thus modify the confinement of the field to extend the tail further.

This suggestion was discussed by Dessler (1964) in a study of the length of the magnetospheric tail. He concluded that the minimum length would be 100 R_E (R_E=Earth Radius = 6378.1 Km) and examining possible sources of internal pressure concluded that hydromagnetic wave radiation pressure alone was adequate to prevent the tail from closing before the termination of the solar wind, at 20 to 50 AU. Dungey (1965) regarded such length estimates as unreasonable and suggested that 100 R_E was probably more nearly correct.

Experimental studies of the distant geomagnetic field in the context of the geomagnetic tail were begun by the Explorer 6 satellite (Smith et al., 1960: Sonett et al., 1960) in 1959 with detailed mapping of two components of the geomagnetic field between 2-7.5 R_E. The measurements from Explorer 6 were performed over an azimuth range relative to the earth-sun line of approximately 60^o to 150^o West. Large decreases in the magnetic field were detected at great distance from the earth and were initially interpreted as representing the magnetic effects of a large scale permanent ring current located at a geocentric distance of 10 R_E.

In 1961 the Explorer 10 spacecraft performed vector magnetic field measurements from 2 to 40 R_E along a trajectory at approximately 135^o West of the earth-sun line. A significant distortion of the geomagnetic field was observed beyond 10 R_E (Heppner et al., 1963) with an increased magnitude and a steady orientation noted. No evidence was found for the previously reported ring current. Subsequent re-examination of the earlier Explorer 6 data (Smith, 1962: Smith et al., 1964) indicated that those results were consistent with data from Explorer 10 only within the framework of an extended geomagnetic tail field on the night side of the earth.

From measurements of energetic particles on Explorer 12 Freeman (1964) concluded that there existed a strong day night asymmetry in the spatial distribution of energetic electrons at altitudes less than 13.1 R_E. The first geocentric satellite to provide almost a full one year study of the earth's environment was Explorer 14 in 1962-1963, with an apogee of 15.9 R_E.

An enhancement on the night side of the earth as shown in Figure 2 was studied by Frank (1964). On the same satellite, Cahill (1964a) detected a strong distortion of the geomagnetic field near the midnight meridian plane both in direction and magnitude. A summary of these results is presented in Figure 3 (Cahill, 1966) which shows the non-dipolar geometry of the observed geomagnetic field. These results suggested the existence of a tail to the magnetosphere but did not provide data from sufficiently large distances to detect the fully developed geomagnetic tail.

Preliminary results from the Vela satellite on the distribution of energetic electron fluxes on the night side of the earth at a geocentric radial distance of 16 R_E were presented by Singer et al., (1965). These data confirmed the earlier results obtained indicating the existence of an enhanced particle flux on the night side of the earth and suggested that this broad region extended from the boundary of the trapped radiation belts to satellite apogee-perigee, both $\sim$ 16 R_E.

On the basis of these experimental results, Axford et al., (1965) and Dessler and Juday (1965) proposed separate models of the formation of a permanent geomagnetic tail. The significant difference in the two models, shown in Figure 4, is the prediction of a plasma - magnetic neutral sheet and merging at a neutral line in the work of Axford et al., as shown in the upper diagram. Beyond the neutral line, the direction of the component of the magnetic field perpendicular to the neutral sheet reverses direction.

Dessler and Juday (1965) proposed a model for the geomagnetic tail with negligible merging based upon the argument that the conductivity of the plasma was sufficiently high to inhibit merging and annihilation of field lines. Their model is shown in the lower half of Figure 4 in which the neutral sheet is represented by the horizontal line and was proposed to extend to the termination of the solar wind boundary. The geometry of the tail transverse to the tail axis was suggested by both groups to be in the form of a θ with the horizontal bar representing the surface separating oppositely directed fields.

The existence of a neutral line in the geomagnetic tail was suggested earlier by Dungey (1961). In studying the results of the Pioneer 5 magnetic field experiment, which indicated the existence of an interplanetary magnetic field component perpendicular to the ecliptic plane (Coleman et al., 1960), Dungey concluded that there would be two characteristically different configurations to the geomagnetic field as the result of the interconnection of interplanetary and geomagnetic field lines. In the case of oppositely directed fields, a neutral point developed on the sunward side of the earth and a neutral line on the night side.

In a recent review of the large scale electric field in the magnetosphere, Obayashi and Nishida (1968) have summarized the various theoretical models which have been proposed for the magnetosphere. The distinguishing feature of the different models is based upon whether or not the magnetosphere is electrically shielded from interplanetary space so that bulk motion of plasma across the magnetopause

is prohibited. Both of the models shown in Figure 4 correspond to a shielded magnetosphere in which the effect of the interplanetary magnetic field is ignored. Unshielded models of the magnetosphere have been proposed by Alfvén (1964) and Dungey (1963) in which the interplanetary electric field is imposed on the magnetosphere.

The mechanism for the formation of the geomagnetic tail similarly differs between the models proposed. Axford and Hines (1961) proposed that a viscous-like interaction is effective on the magnetosphere boundary for momentum transfer from the solar wind. This then extends the geomagnetic field on the night side of the earth. In the case of the model of Dungey and Levy, Petschek and Siscoe (1964), merging of the interplanetary and geomagnetic fields occurs on the sunlit hemisphere of the magnetosphere and field lines are carried convectively to the night side of the earth forming the extended geomagnetic tail. Parker, (1967) has studied the equilibrium of the magnetopause boundary and concluded that no stable configuration is possible on a small length scale. This nonequilibrium leads to a mixing of geomagnetic lines of force with the solar wind and thus produces a 'viscous' drag as the plasma flows along the magnetopause. The erosion of field lines proceeds at a rate whereby the entire tail would be formed in only 10^3-10^5 seconds. For earlier reviews of the theory of the magnetosphere and related experiments the reader is referenced to the work of Obayashi (1964) and Cahill (1964b).

Results from IMP-1: 1964

A comprehensive survey of the geomagnetic field boundary, detailed measurements mapping the earth's magnetic tail and the discovery of the imbedded neutral sheet were performed in 1964 by the IMP 1 satellite (Ness, 1965). These data showed that the geomagnetic field extended out far out behind the earth to satellite apogee, 31.4 R_E, a distance half way to the moon. A sample of the measurements obtained is shown in Figure 5 from orbit number 41, that orbit closest to the midnight meridian plane. The results are presented in solar ecliptic coordinates and demonstrate the remarkable feature that beyond 12 R_E the magnetic field is oriented parallel to the earth-sun line ($\theta = 0^o$; $\phi = 0^o$, 180^o) with sense either towards ($\phi = 0^o$) or away ($\phi = 180^o$) from the sun depending upon whether or not the satellite is above or below a magnetically neutral surface identified as the neutral sheet.

The magnetic neutral sheet was observed to be relatively thin, on the scale of a fraction of an earth radius thick. It should be noted that it is not possible from a single satellite observation to uniquely determine a separation of space and time variations without an a priori assumption as to the invariance of either the structure or the motion. In addition it is necessary to consider the model of the field reversal which is used to determine the effective thickness of the region. The dashed lines in this figure represent the theoretical geomagnetic field extrapolated using a simple geocentric dipole.

The presence of a field reversal implies the existence of a plasma sheet and an electric current associated with the spatial gradient of the magnetic field. A detailed study of the IMP 1 neutral sheet crossings by Speiser and Ness (1967) has yielded the equivalent current magnitude and direction necessary to form a physically consistent model of the field reversal. These currents are derived from the curl of the magnetic field, $\vec{J} = \nabla \times \vec{H}$, with the assumption that the geometry of the neutral sheet is a two dimensional sheet.

An interesting feature of these observations has been the identification of multiple crossings of the neutral sheet during a single satellite pass. This is interpreted to represent motion of the neutral sheet relative to the satellite. Inspection of Figure 5 will show that on May 3 at a distance of 28 R_E (at 0600) the neutral sheet probably passed over the satellite twice within one hour. On occasions, individual crossings of the neutral sheet are observed to occur at 24 hour intervals. This can be readily understood in terms of the diurnal motion of the earth's magnetic dipole axis and the accompanying oscillation of the orientation of the neutral sheet.

In order to take these factors into account, Ness (1965) introduced a solar magnetospheric coordinate system in which the XZ plane is determined by the earth-sun direction and the magnetic dipole axis of the earth. A summary of the vector measurements obtained by the IMP 1 satellite in the geomagnetic tail are shown in Figure 6. The position of the neutral sheet crossings on orbits 44-47 are also indicated. These data show that the neutral sheet will be located

above the solar magnetospheric equatorial plane in the northern hemisphere summer and correspondingly below it in the winter. This is because the origin of the neutral sheet does not begin at the earth but at the geomagnetic equator at a distance of approximately 10 R_E (Murayama, 1966; Russell and Brody 1967; Speiser and Ness 1967). It is presently believed that the neutral sheet is generally approximately parallel to the solar magnetospheric equatorial plane but located at a distance from the plane which depends upon the "angle of attack" of the solar wind on the geomagnetic field, χ_{SS}.

Particle measurements on the IMP 1 satellite by Anderson (1965) showed the existence of intense transient bursts of electron fluxes ($E_e > 45$ kev) with rapid rise and slow decay. In the spatial analysis of the frequency of occurrence of these events, called electron islands, he concluded that it decreases with increasing distance down the geomagnetic tail axis. Murayama (1966) in a separate analysis of electron fluxes ($E_e >160$ kev) measured on the same satellite, was not able to confirm this radial dependency. Because the satellite motion radially was so highly correlated with the motion transverse to the neutral sheet, he concluded that these events tended to occur more frequently closer to the neutral sheet.

A sample of the electron island events observed by IMP 1 is presented in Figure 7. Simultaneous measurements with the magnetic field are also shown and indicate that frequently the electron events are associated with large depressions of the magnetic field. A calculation of the diamagnetic effects of the observed electrons shows that they

represent about only one percent of the plasma energy required to decrease the magnetic field strength by the observed value. Thus evidence is obtained that the island events are due to electrons with energy considerably below the 45 kev threshold of the geiger counters instrumented for these satellites. The source of these particles is unknown. They could represent radiation belt particles lost to the tail, or accelerated in the tail by merging at the neutral sheet or entry from interplanetary space into the tail at large distances from the earth. Cahill (1966) suggested that the large scale decrease of field strength on the night side of the earth between 8-12 R_E represents the inflation of the magnetosphere due to the contained plasma.

Correlative studies of the variation of the radiation belt boundaries and the geomagnetic tail have also been conducted (Ness and Williams, 1966). From direct measurements of the invarient latitude of the boundary of trapped radiation it has been concluded that during geomagnetic storms a motion of the trapping boundary to lower latitudes is accompanied by an increase in the geomagnetic tail field strength. The particular event studied, shown in Figure 8, was a geomagnetic storm in which the magnetic tail field strength approximately doubled, from 15 to 30 gammas, following the sudden commencement.

At the time of the sudden commencement the boundary of the magnetospheric tail was observed to move in past the satellite briefly. This determined the size of the geomagnetic tail and yielded an estimate

of the total contained magnetic flux. Combined with the observations of the invariant latitude boundary motion, it was concluded that the increased magnetic field strength of the geomagnetic tail was due to compression by the plasma in the magnetosheath and also the addition of new lines of force which were extended into the tail during this storm event. All storm effects observed by IMP 1 in 1964 in the geomagnetic tail were compared with corresponding terrestrial observations and a high correlation was found between tail field magnitudes and the planetary magnetic activity index Kp (Behannon and Ness, 1966).

Correlated measurements of the response of the magnetosphere and tail, observed by OGO-1, to an impinging interplanetary shock, observed by IMP-3 and Explorer 33 (Ness and Taylor, 1967), have been compared by Sugiura et al., (1968). This analysis suggests that the disturbance observed in the tail, a sudden increase, is due to a hydromagnetic wave propagating within the magnetosphere and adding new magnetic flux to the tail.

Formation and General Shape of the Tail

Significant measurements of the outer geomagnetic field demonstrating the gradual formation of the geomagnetic tail in the dawn to midnight region of the magnetosphere were performed by IMP 2 (Fairfield and Ness, 1967). Figure 9 presents a summary of these measurements with the nonradial nature of the field vectors in the lower half of the figure illustrating how the field is swept back by the solar wind and the tail formation is begun. From these observations it appears that an entire magnetic field meridian plane is distorted and deflected backwards into the geomagnetic tail. Hypothetical meridian planes are sketched in as dashed lines.

Data obtained for regions 5 through 8 thus formed are shown in the upper portion of the figure. Here the radial nature of the field is observed in sectors 7 and 8 as well as the existence of the field reversal region in sectors 5 and 6. These data demonstrate directly the formation of the field reversal region as close to the earth as 8 R_E, in agreement with the earlier interpretations of the IMP 1 measurements.

Extensive measurements of the geomagnetic tail and its boundaries out to distances of 80 R_E, well beyond the orbit of the moon, have been performed by Explorer 33 (Ness et al., 1967a; Behannon, 198; Mihalov et al., 1968). This satellite represented an attempt by the USA to orbit the moon which failed and was placed instead into a very high apogee

earth orbit. During the first five months apogee varied between 70-80 R_E with perigee varying between 8-15 R_E due to perturbations by the gravitational field of the moon.

Mapping of the distant magnetosheath, bow shock wave and geomagnetic tail from the dawn flank of the earth's bow shock to the dusk flank extended beyond the lunar orbital distance of 60 R_E. A summary of the boundaries of the geomagnetic tail observed by Explorer 33 is shown in Figure 10. It is noted that multiple observations of the tail boundary are a common feature of the magnetopause observations. This variation can be due to waves propagating on the surface of the magnetopause, the expansion and contraction of the entire magnetosphere in response to a varying solar wind flux or a change in the relative position or aspect of the boundary due to a varying angle between the earth's magnetic dipole axis and the solar wind velocity.

An attempt to sketch in average boundary positions has been made and illustrates the asymmetry observed in these data. A separate analysis of these observations in planes transverse to the X_{SE} axis has indicated that the geometry of the geomagnetic tail transverse to its axis is not cylindrical but rather elongated in a direction perpendicular to the solar magnetospheric equatorial plane. The distance from the tail axis to the magnetopause is estimated to be approximately 50% greater in a direction perpendicular to the neutral sheet than the distance of approximately 20 R_E in the neutral sheet. This asymmetry is in agreement with the model of the geomagnetic tail proposed by Axford et al. (1965) and Dessler and Juday (1965).

Typical measurements in the geomagnetic tail are shown in Figure 11. The lower portion of the figure presents 24 hours of data obtained during a particularly quiet time when the planetary magnetic activity index was 0, 0, 0, 1, 1, 0+, 0+, 0+, and shows how very steady the geomagnetic tail field can be. These data represent the average magnetic field and its RMS deviation computed from 16 individual vector measurements at 5.12 second intervals. The energy present in the magnetic field fluctuations is less than one percent of the ambient steady magnetic field energy density. Note that throughout the 24 hour interval covered in this diagram there appears to be no evidence for modulation of the field magnitude or orientation due to the wobble of the nonaxial geomagnetic dipole.

The upper portion of Figure 11 illustrates a more disturbed time in the geomagnetic tail when the magnetic activity index rose from 1-, 0+, 1, 1, 1 to 3+, 3, 4+. Preceding the sudden commencement storm at 1502 UT an interval of magnetic field magnitude fluctuations is observed with very long period, approximately 20 minutes. These are also observed to be present after the sudden commencement which has a rise time of approximately 8 minutes. Note that at 1720 the field orientation as measured by $\emptyset$ changes abruptly. Comparison of simultaneous plasma data with the MIT group has revealed the motion of the magnetopause boundary past the satellite at this time in response to varying solar wind conditions.

A recent theoretical study by Smit (1968) has shown that the eigenmodes of the magnetosheath-magnetosphere system include long low frequency periods of 6-7 minutes.

Studies of the natural resonances of the geomagnetic tail have been conducted by McClay and Radoski (1967) and Patel (1967). Assuming that the tail is represented by a cylindrical wave guide of radius 40 R_E, density $5p/cm^3$ and B = 40γ, with reflecting walls and neutral sheet, McClay and Radoski deduce that the lowest periods are on the order of 20-35 minutes for TM or TE modes. Patel's study (1967) assumes a double cylinder geometry, each of radius 7 R_E, density $=1p/cm^3$ and B = 10 gammas. He concludes that eigen-periods of the order 24-32 minutes represent the mixed transverse and longitudinal mode, in agreement with observations. These studies suggest that the tail itself is the source of these observed long period fluctuations.

A summary of the geomagnetic tail observations obtained by Explorer 33 during orbits 1 through 8 is shown in Figure 12. The hourly average vectors were obtained by linearly averaging the previously referenced 82 second averages of the magnetic field components. The average solar magnetospheric components are projected onto the X_{SM}-Z_{SM} and Y_{SM} planes with as many data points shown as possible to prevent excessive overlapping. In the upper portion of the figure the field reversal region is well-defined and a gradient of the field magnitude is evident along the geomagnetic tail. The lower two figures suggest possibly a skewing of the field vector although this is spurious due to the use of an incorrect spin axis orientation of the spacecraft during initial phases of data analysis (Behannon, 1968).

Tail Field Gradient and Neutral Sheet Merging

An important result of the mapping of the geomagnetic tail by Explorer 33 has been the determination of a general decrease in tail field magnitude with distance down the tail. Figure 13 summarizes average field magnitudes as a function of distance along the earth-sun line. Data from a total of 740 hours during which Explorer 33 was clearly in the tail was subjected to a multiple correlation and regression analysis (Behannon, 1968). In this study, the hourly average field magnitude is the dependent variable and independent variables are the distance, X_{SE}, of the spacecraft down the tail, the magnetic activity index, Kp, and the perpendicular distance, Z_{SM}, of the satellite from the solar magnetospheric equatorial plane. The best correlation obtained was between field magnitude and distance down the tail and with decreasing coherency the planetary magnetic activity index Kp and finally transverse distance from the neutral sheet Z_{SM}. Behannon (1968) has found that $|B| \alpha |X_{SE}|^{-0.3 \pm 0.2}$ with a standard deviation of 3.1 gammas (See Figure 13).

Several different formulations have been obtained by other workers (Mihalov et al., 1968) with a similar experiment on the same spacecraft and are summarized in the following equations:

$$|B| = (191.4 \pm 14.2)\ R^{-0.736 \pm 0.019}$$

$$|B| = (26.8 \pm 2.2)\ \exp\left(-\frac{R}{59.4 \pm 4.9}\right)$$

where R represents the distance down the tail in earth radii.

The field magnitudes predicted by the regression curve for the interval between -10 R_E and -30 R_E are consistent with the median tail field magnitude of 16 gammas found earlier by the IMP 1 satellite in that region.

The observed field magnitude gradient in the tail can result either from an increase in the cross sectional area of the tail with distance down the tail and/or by reconnection of field lines across the neutral sheet. Earlier analyses by Speiser and Ness (1966) concluded that up to 30 R_E the average field component transverse to the neutral sheet plane is northward. The data obtained by Behannon (1968) is not conclusive regarding the sense of the transverse component beyond 30-50 R_E due to variations in the polarity.

The occurrence of both northward and southward components transverse to the neutral sheet were interpreted by Mihalov et al., (1968) as indicating that magnetic field loops are observed crossing the field reversal region. In the analysis of their data obtained on Explorer 33 they conclude that statistically a southward component is observed when the satellite is beyond 60 R_E.

In a study of IMP 3 observations of the geomagnetic tail field and neutral sheet at distances to 40 R_E (Speiser and Ness, 1967), it was suggested that caution be exercised in reaching conclusions regarding the northward or southward directed sense of the magnetic field near the field reversal region. This is due to the a prior unknown orientation of the neutral sheet and the effect this has upon the

attempt to determine the component transverse to the neutral sheet. Indeed, it appeared at times from IMP 3 that the neutral sheet was tipped by as much as 30^{o} from being parallel to the solar magnetospheric equatorial plane. Thus it is believed to be premature in concluding that the neutral line in the geomagnetic tail is present at 30-60 R_E.

PLASMA SHEET OBSERVATIONS

Early measurements by Gringauz et al., (1960) and Freeman (1964) suggested the presence of electrons of low energy (Ee> 200 eV) at large distances on the night side of the earth well beyond the Van Allen radiation belts. The most comprehensive observations of the plasma sheet in the geomagnetic tail have been performed by the Vela series of satellites (Singer et al., 1965 : Montgomery et al., 1965). These studies have shown that energetic electrons (E>45 kev) when observed in the magnetotail are normally observed simultaneous with low energy electrons (E<20 kev) although it is possible to observe low energy electrons in the absence of high energy electrons (Bame et al., 1966).

Discussion of the Vela satellite program and associated instrument and spacecraft details have been presented by Singer (1965), and Coon (1966). Examples of the electron spectrum measured at different times by Vela in the magnetosheath and plasma sheet are shown in Figure 14. The average energy of each spectrum is approximately determined by the spectral peak.

Results obtained from a typical pass through the geomagnetic tail are shown in Figure 15. Prior to 0700 the electron flux is below the detectable limit of the instrument, 10^7 cm^2/sec, omni-directional for Ee<200 eV and 10^3 cm^2/sec for E> 45 kev. For the remainder of this data the spacecraft appears to have been imbedded in the plasma sheet, as evidenced by the low energy electron flux. The variations of the

electron-flux (E> 45 kev) in this data show the similar fast rise and slow decay characteristics that were described as electron islands observed by IMP 1 by Anderson (1965).

Examples of the differential energy spectra obtained at the lettered times in Figure 15 are shown in Figure 16. It is seen that the energy distributions are generally broader than a Maxwellian with a super-thermal high energy tail that can be fitted with a negative exponent power law spectrum. Montgomery (1968) has shown that during disturbed times the assumption of a power-law spectrum for Ee> 40 kev is better than a Maxwell-Boltzman while during quiet times the opposite is true. The average energy of the spectra in Figure 16 for this time interval range from 1 to 7 kev while number densities range from .1 to .3/cm^3. A computation of the equivalent magnetic field intensity assuming equipartition of energy between the electron component of the plasma and the positive component yields field magnitudes of approximately 18 to 20 gammas. These results are in excellent agreement with separate measurements by IMP 1 of the magnetic field strength in this region of space.

While located in the magnetotail the observations of the positive component of the plasma have been intermittent due to their low flux level. During these limited observations proton number densities are found of approximately the same value as the electron number density with average energies ranging to above 10 kev.

Extensive measurements of the spatial distribution of the plasma sheet have shown that the electrons between 15.5 and 20 R_E occupy a thick sheet or slab stretching across the geomagnetic tail. The plasma

sheet thickness observed near the midnight meridian plane is approximately 4 to 6 R_E although the sheet appears to flare out by about a factor of 2 near the boundaries of the geomagnetotail.

The plane of symmetry of the plasma sheet appears to lie midway between the solar magnetospheric and geomagnetic equatorial planes. This shows the significant effects of the geomagnetic dipole orientation at this distance. Thus depending upon the season of the year the plasma sheet will be found either above or below the solar magnetospheric equatorial plane, as was determined from the IMP 1 magnetic field data for the field reversal region.

A summary of the Vela data spatial distribution interpretation and region covered in the geomagnetic tail is shown in Figure 17. These results nicely compliment the separate results obtained by the IMP 1 magnetic field measurements in establishing the general yearly variation of the plama sheet orientation and the balance of magnetic and plasma pressure, which may be due to local acceleration mechanisms. In Montgomery's study (1968) of the detailed spatial distribution of energetic electron fluxes, Ee>40 kev, he concluded that they do not form a continuous non-thermal high energy tail but represent a second population with a maximum flux at ≈10 kev. These fluxes are found to occur most often on the dawn side of the magnetosphere.

The first joint measurements of the magnetic field and plasma sheet of the geomagnetic tail were performed on the out bound pass of the heliocentric space probe Pioneer 7 in 1966 (Lazarus et al., 1968). A summary of the spatial distribution of the observations transverse to the earth-sun line is shown in Figure 18. The variation in distance

from the solar magnetospheric equatorial plane, as measured by Z_{SM}, is due to the diurnal wobble of the geomagnetic dipole axis. Observation of electron fluxes are indicated on the trajectory. Note that the neutral sheet is predicted to be observed near 0145 and subsequently at approximately 1845 on the basis of an ideal sheet model.

Experimental observations obtained are shown in Figure 19. Typical electron densities are observed of approximately $0.5/cm^3$ with most probable speeds of approximately 10^4 km/sec, corresponding to an electron energy density of about 250 electron volts/cm^3. For this experiment protons of the same energy and concentration will occur a factor of 4 below the detectable threshold of the instrument.

Significant variations of the electron flux and magnetic field magnitude are observed in anticorrelation. This aspect of the results is emphasized in the lower portion of the figure where the total plasma plus magnetic pressure is presented. It has been assumed that the unmeasured proton pressure is equal to the electron pressure. Note that the total pressure remains nearly constant during those intervals when there are significant variations of either field or electron flux. There are, however, significant variations in the total pressure which are assumed to reflect variations in external conditions in the magnetosheath.

A self-consistency arguement has been employed to study the proton pressure for intervals when the total pressure is approximately constant, from 0000 to 0630 and 0700 to 0930. The results obtained suggest that

the proton pressure is a factor of 1.2 to 2.8 times the electron pressure. Transitions between low B high P regions and high B low P regions appear to be a distinguishing feature of these data suggesting a sharp boundary to the plasma sheath.

Simultaneous with the loss of detectable electron flux from 0930 to 1545 is the geomagnetic bay activity recorded at College, Alaska. Bay associated decreases in the geomagnetic tail field magnitude have also been observed by OGO-1 (Heppner et al., 1967). Qualitatively and roughly quantitatively these observations agree with the collapse rebuild theories that have been suggested in various forms by Atkinson (1966), Axford (1965) and Dungey (1965) whereby a tail implosion at the neutral sheet feeds energy to the bay disturbance.

Various processes accellerating particles in the neutral sheet have ranged from steady-state acceleration as studied by Speiser (1966), to a flare type mechanism in the tail as suggested by Piddington (1967). In this model rapid annihilation of field lines across the neutral sheet would feed energy to particles and accelerate them to possibly auroral energies. This suggestion requires that merging take place sporadically in the tail. Coppi et al. (1966) have studied the stability of the neutral sheet region in the context of the Furth et al.,(1963) tearing mode finite resistivity instability. Murayama and Simpson (1968) have recently completed a detailed study of the correlation of IMP-1 magnetic field data neutral sheet crossings and electron fluxes. It was found that the peak flux (Ee>160 kev) occurs at the field reversals found by Speiser and Ness (1966) and that fluxes are continuously

present. Two possible sources are:

(a) The neutral sheet is well-connected, for particle propagation, to a region of the magnetosphere where the acceleration of electrons occurs or

(b) the electrons are accelerated in the neutral sheet.

Detailed magnetic field components and RMS deviations obtained by the Pioneer 7 passage through the neutral sheet are shown in Figure 20. It is seen here that the field component B_{ZSM} transverse to the neutral sheet is several gammas northward. Note that in the neutral sheet region, rapid fluctuations of the magnetic field up to 5 cps, the upper pass band of the instrument, are observed. These data show that electromagnetic noise is present at the field reversal in the core of the plasma sheet.

On the lunar orbiting spacecraft Luna 10, Gringauz et al. (1966) reported upon the detection of the plasma sheet in the geomagnetic tail at lunar distances. However on the same spacecraft Dolginov et al. (1966) did not obtain a clear indication of the existence of the Earth's tail. Ness (1967) has suggested that the apparent data inconsistency is due to the immersion of the Luna 10 spacecraft in the plasma sheet, when weak and variable direction fields would be expected rather than a well-defined tail field geometry.

The Distant Geomagnetic Tail

While earth orbiting spacecraft have shown that the tail extends to the distance of the moon's orbit and beyond, still being well-defined at 80 R_E, the first opportunity to detect the tail far downstream at 3300 R_E by Mariner 4 was not successful (Van Allen, 1965). The next opportunities were provided by the Pioneer 7 and 8 heliocentric space probes whose orbits are shown in Figure 21. Throughout the interval on Pioneer 7 from September 5 to 30 the orientation of the interplanetary field was observed infrequently to closely parallel the earth-sun line (Ness et al., 1967b). Simultaneous with these observations, anomalous plasma flow conditions were detected by Wolfe et al. (1967). At no time during the observations was a fully developed geomagnetic tail and imbedded neutral sheet observed as proposed by Dessler (1964).

A sample of the results obtained from detailed measurements by Pioneer 7 is shown in Figure 22. Field orientations of approximately $\phi=180^o$, $\theta=0^o$ indicating anti-solar directed fields from the southern hemisphere of the geomagnetic tail were detected for limited times during this two hour interval. These were associated with anamolous plasma conditions as indicated. Generally throughout this interval, the geomagnetic tail field is identifiable by its orientation and field magnitude of approximately 8 gamma.

It is believed that at these large distances the geomagnetic tail is no longer composed of only two distinct bundles of oppositely directed field lines separated by a single neutral sheet. The tail is thought

to be separated into a number of filaments in close proximity, possibly intertwined, which while still maintaining direct connection to the earth no longer preserve the well-defined θ cross section tail geometry observed in cis-lunar space.

If one extends beyond 80 R_e the computed regression curves of field magnitude gradient shown in Figure 13, it is found that the magnitude will decrease to a value of 4 gammas between 125-175 R_E during times of low Kp. On this basis, the tail is less well-defined beyond approximately 200 R_E since the tail field magnitude decreases to the quiet time interplanetary level at that distance. Fairfield (1968) has compared simultaneous data from cislunar-space and Pioneer 7 and suggests that a filamentary model of the tail is not necessarily a unique interpretation, due to the variability of the observed magnetic fields, and that a coherent tail might be present at 1000 R_E.

More recently observations by the Pioneer 8 spacecraft at a distance of approximately 500 R_E have been performed. The results obtained yield a similar interpretation to that of Pioneer 7. The geomagnetic tail is not well-defined at 500 R_E as a simple coherent θ geometry but appears to be represented by many separate filaments (Mariani and Ness, private communication).

Summary

During the past seven years, experimental investigations of the earth's magnetic tail and imbedded neutral sheet have established its permanent existence as an extension of the magnetosphere with lines of force closely paralleling the earth-sun line. Oppositely directed field lines are separated by a field reversal region approximately .1 to 1 R_E thick and frequently in motion. The plasma sheet surrounding the neutral sheet appears to be thicker, up to 4-6 R_E in the center of the tail, flaring to approximately twice that near the dusk and dawn magnetopause boundarys.

The geomagnetotail is still well-defined out to radial distances of 80 R_E although at distances of 500 and 1000 R_E it appears to have broken up into separate filaments. The tail does not appear to be cylindrical in shape, having a width of approximately 40 R_E in the plane of the neutral sheet and approximately 60 R_E in the perpendicular direction. Multiple correlation and regression analysis shows that the field magnitude decreases from approximately 16 gamma at 20 R_E to 7 gammas at 80 R_E. Impulsive field magnitude decreases have been observed in the magnetic tail in association with transient electron events. The occurrence of these electron bursts decreases with the distance from the neutral sheet. The injection of these particles into the geomagnetic tail has recently been studied by the Lunar Explorer 35 spacecraft with the moon used as an occulting disk. Both Lin (1968) and Van Allen and Ness (1968) have concluded, from quite different physical view points, that the electron events observed in the geomagnetic tail are due to injection into the tail at a distance beyond the moon.

Geomagnetic storms have been observed in the tail in correlation with world wide terrestrial disturbances. Typically the tail field magnitude increases by a factor of 2 or more during the main phase of the sudden commencement storm. The magnitude increase is due to both a compression of the magnetosphere tail and the addition of magnetic flux from the magnetosphere as polar cap regions expand to lower latitudes.

Theoretical studies of the mechanism responsible for the formation of the geomagnetic tail have not yet reached agreement. One theory requires a viscous-like interaction on the boundary of the magnetosphere to transfer momentum to the geomagnetic field and exert the stresses necessary to extend field lines down-stream as the solar wind flows past the earth. A second model proposes the existence of rapid merging of field lines on the sun-lit hemisphere of the magnetosphere and subsequent convection of connected interplanetary and geomagnetic field lines to form the geomagnetic tail.

Agreement now does seem to be reached in the area of merging of field lines across the neutral sheet. Dessler (1968), on the basis of experimental studies of the plasma sheet, has recently re-assessed his theoretical model proposed earlier which predicted no merging in the geomagnetic tail. The lower portion of Figure 23 presents the modified model with merging occuring at the neutral line, which is proposed to exist at a distance of about 15 R_E beyond the earth. The recent results from Explorer 33 (Mihalov, 1968) may give support to the idea that the neutral line has been crossed somewhere between 30-60 R_E behind the earth. For completeness, a diagram of the

geomagnetic tail discussed by Piddington (1967), expanding upon his earlier discussions, is presented in the upper portion of Figure 23.

Outstanding Problems

Future studies of the geomagnetic tail will be directed to resolution of the following major questions:

1. What mechanism forms the geomagnetic tail?
2. At what distance behind the earth does the coherent well-ordered tail cease to exist?
3. Is merging of field lines across the neutral sheet a continuous or impulsive process and where does this take place?
4. Are auroral particles accelerated by flare-like processes in the geomagnetic tail?
5. What is the source of the energy and by what processes are electrons accelerated to form the fluxes observed both in the neutral sheet and the tail?

It is possible that continued analysis of available spacecraft results may answer these questions. Simultaneous observations of both the geomagnetic tail and interplanetary medium are now being studied so that the time sequence of events regarding the response of the magnetosphere and tail to propagating disturbances in the solar wind can be established. In an overview of our solar system, among the moon and planets it appears that the earth and probably Jupiter are unique in possessing long magnetic tails due to the intrinsic magnetic planetary field. While the corresponding field geometry for Venus

and Mars is not well known it appears that their aft-flow pattern may more closely resemble that of the moon where a wake is formed rather than a distinctive tail.

Acknowledgement

I am pleased to acknowledge the important participation in the research reported here of my colleagues Mr. K. W. Behannon and Drs. D. H. Fairfield and T. W. Speiser.

References

Alfven, H. A., Hydromagnetics of the magnetosphere, Space Sci. Rev., 2, 862-870, 1963.

Anderson, K. A., Energetic electron fluxes in the tail of the geomagnetic field, J. Geophys. Res., 70, 4741-4763, 1965.

Anderson, K. A. and N. F. Ness, Correlations of magnetic fields and energetic electrons on the IMP 1 satellite, J. Geophys. Res., 71, 3705-3727, 1966.

Atkinson, G., A theory of polar substorms, J. Geophys. Res., 71, 5157, 1966.

Axford, W.I., Magnetic storm effects associated with the tail of the magnetosphere, paper presented as ESRO Conference on the magnetosphere, November 1965.

Axford, W.I., and C. O. Hines, A unifying theory of high latitude geophysical phenomena and geomagnetic storms, Can. J. Phys., 39, 1433, 1961.

Axford, W. I., H. E. Petschek, and G. L. Siscoe, The tail of the magnetosphere, J. Geophys. Res., 70, 1231-1236, 1965.

Bame, S. J., J. R. Asbridge, H. E. Felthauser, R. A. Olson, and I. B. Strong, Electrons in the plasma sheet of the earth's magnetic tail, Phys. Rev. Letters, 16, 138-142, 1966.

Bame, S. J., J. R. Asbridge, H. E. Felthauser, E. W. Hones, and I. B. Strong, Characteristics of the plasma sheet in the earth's magnetic tail, J. Geophys. Res., 72, 113-129, 1967.

Behannon, K. W., Mapping of Earth's Bow Shock and Magnetic Tail by Explorer 33, J. Geophys. Res., 73, 907-930, 1968.

Behannon, K. W. and N. F. Ness, Magnetic storms in the earth's magnetic tail, J. Geophys. Res., 71, 2327-2351, 1966.

Cahill, L. J., Preliminary results of magnetic field measurements in the tail of the geomagnetic cavity, IG Bull., 79, Trans. Am. Geophys. Union, 45, 231-235, 1964

Cahill, L. J. Jr., In "Space Physics" (D.P. LeGalley and A. Rosen, eds.) p. 301. John Wiley and Sons, New York, 1964b.

Cahill, L. J., Inflation of the magnetosphere near 8 earth radii in the dark hemisphere, Space Research VI, 662-678, 1966.

Coleman, P. J., L. Davis, and C.P. Sonett, Steady component of the interplanetary magnetic field, Pioneer 5, Phys. Rev. Letters, 5, 43-46, 1960.

Coon, J., Vela satellite measurements of particles in the solar wind and the distant geomagnetosphere, Radiation Trapped in the Earth's Magnetic Field, ed. B. M. McCormac, p. 231, D. Reidel, Dordrecht, Holland, 1966.

Coppi, B., G. Laval and R. Pellat, Dynamics of the geomagnetic tail, Phys. Rev. Letters, 16, 1207-1210, 1966.

Dessler, A. J., Length of the magnetospheric tail, J. Geophys. Res., 69, 3913-3918, 1964.

Dessler, A. J., Magnetic merging in the magnetospheric tail, J. Geophys. Res., 73, 209-214, 1968.

Dessler, A. J., and R. D. Juday, Configuration of auroral radiation in space, Planetary Space Sci., 13, 63-72, 1965.

Dolginov, Sh. Sh., E. G. Yeroshenko, L. H. Zhuzgov and N. V. Pushkov, Measurements of the magnetic field in the vicinity of the moon on the AMS Luna 10, Doklady A. N. SSSR, 170, 574-577, 1966.

Dungey, J. W., Interplanetary magnetic field and the auroral zones, Phys. Rev. Letters, 6, 47, 1961.

Dungey, J. W., The Structure of the Exosphere or Adventures in Velocity Space, in Geophysics: The Earth's Environment (ed. by C. Dewitt et at.) pp. 505-552, Gordon and Breach, New York 1963.

Dungey, J. W., The length of the magnetospheric tail, J. Geophys. Res., 70, 1753, 1965.

Dungey, J. W., Theory of the quiet magnetosphere in "Solar Terrestrial Physics," (J. W. King and W. S. Newman, eds.) p. 91-106, Academic Press, New York, 1968.

Fairfield, D. H., Simultaneous measurements on three satellites and the observation of the geomagnetic tail at 1000 R_E, NASA-GSFC preprint X-612-68-124, 1968.

Fairfield, D. H. and N. F. Ness, Magnetic field measurements with the IMP 2 satellite, J. Geophys. Res., 72, 2379-2403, 1967.

Frank, L. A., A survey of electrons beyond 5 R_e with Explorer 14, J. Geophys. Res., 70, 1593-1626, 1965.

Freeman, J. W., Electron distribution in the outer radiation zone, J. Geophys. Res., 69, 1691-1724, 1964.

Furth, H. P., Prevalent instability of nonthermal plasmas, Phys. Fluids, 6, 48-57, 1963.

Gringauz, K. I., V. G. Kurt, V. I. Moroz, and I. S. Shklovsky, Results of observations of charged particles observed out to 100,000 km with the aid of charged particle traps on Soviet space probes, Astron. Zh., 37-4, 716-735, 1960.

Gringauz, K. I., V. V. Bezrukikh, M. Z. Khokhlov, L. S. Musatov and A. P. Remizov, Signs of Crossing by the Moon of the Earth's Magnetosphere Tail According to Data of Charged Particle Traps on the First Artificial Satellite of the Moon, Doklady A. N. SSSR, 170, 570-573, 1966.

Heppner, J. P., N. F. Ness, T. L. Skillman, and C. S. Scearce, Explorer 10 magnetic field measurements. J. Geophys. Res., 68, 1-46, 1963.

Heppner, J. P., M. Sugiura, T. L. Skillman, B. G. Ledley, and M. Campbell, OGO-A magnetic field observations, J. Geophys. Res., 72, 5417, 1966.

Johnson, F. S., The gross character of the geomagnetic field in the solar wind, J. Geophys. Res., 65, 3049-3051, 1960.

Lazarus, A. L., G. L. Siscoe and N. F. Ness, Plasma and magnetic field observations during the magnetosphere passage of Pioneer 7, J. Geophys. Res., 73, 907-930, 1968.

Levy, R. H., H. E. Petschek and G. L. Siscoe, Aerodynamic aspects of the magnetospheric flow, AIAA Journal, 2, 2065-2076, 1964.

Lin, R. P., Observations of lunar shadowing of energetic particles, J. Geophys Res., 73, 3066-3071, 1968.

Mihalov, J. D., D. S. Colburn, R. G. Currie and C. P. Sonett, Configuration and reconnection of the geomagnetic tail, J. Geophys. Res., 73, 943-949, 1968.

McClay, J. F. and H. R. Radoski, Hydromagnetic propagation in a theta-model geomagnetic tail, J. Geophys. Res., 72, 4525-4528, 1967.

Montgomery, M. D., Observations of electrons in the earth's magnetotail by Vela launch 2 satellites, J. Geophys. Res., 73, 871-889, 1968.

Montgomery, M. D., S. Singer, J. P. Conner, and E. E. Stogsdill, Spatial distribution, energy spectra, and time variations of energetic electrons (E> 50 kev) at 17.7 earth radii, Phys. Rev. Letters, 14, 209-213, 1965.

Murayama, T., Spatial distribution of energetic electrons in the geomagnetic tail, J. Geophys. Res., 71, 5547-5557, 1966.

Murayama, T. and J. Simpson, Electrons within the neutral sheet of the magnetospheric tail, J. Geophys. Res., 73, 891-905, 1968.

Ness, N. F., The earth's magnetic tail, J. Geophys. Res., 70, 2989-3005, 1965.

Ness, N. F., Remarks on the interpretation of the Luna 10 magnetometer results, Geomag. and Aero., 7, 433-435, 1967.

Ness, N. F., K. W. Behannon, S. C. Cantarano and C. S. Scearce, Observations of the earth's magnetic tail and neutral sheet at 510,000 kilometers by Explorer 33, J. Geophys. Res., 72, 927-933, 1967a.

Ness, N. F., C. S. Scearce and S. Cantarano, Probable observation of geomagnetic tail at 6 x 10^6 kilometers by Pioneer 7, J. Geophys. Res., 72, 3769-3776, 1967b.

Ness, N. F. and H. E. Taylor, "Observations of the interplanetary magnetic field July 4-12, 1966", NASA-GSFC preprint X-612-67-345, July 1967. Also in Annals of the IQSY, 3, 525-529, (paper 48), 1968.

Ness, N. F. and D. J. Williams, Correlated magnetic tail and radiation belt observations, J. Geophys. Res., 71, 322-325, 1966.

Obayashi, T., Interaction of solar plasma streams with the outer geomagnetic field, J. Geophys. Res., 69, 861-867, 1964.

Obayashi, T. and A. Nishida, Large scale electric field in the magnetosphere, Space Sci. Revs., 8, 3-31, 1968.

Parker, E. N., Small scale nonequilibrium of the magnetopause and its consequences, J. Geophys. Res., 72, 4365-4374, 1967.

Patel, V.L., Magnetospheric tail as a hydromagnetic waveguide, Denver Univ. preprint DU-889-6704, 1967.

Piddington, J. H., Geomagnetic storm theory, J. Geophys. Res., 65, 93-105, 1960.

Piddington, J. H., A theory of auroras and the ring current, J. Atmos. Phys. and Terres. Phys., 29, 87-105, 1967.

Russell, C. T. and K. I. Brody, Some remarks on the position and shape of the neutral sheet, J. Geophys. Res., 72, 6104-6106, 1967.

Singer, S., The vela satellite program for detection of high-altitude nuclear detonations, Proc. IEEE, 53, 1935-1941, 1965.

Singer, S., J. P. Conner, W. D. Evans, M. D. Montgomery and E. E. Stogsdill, Plasma observations at 10^5 km, Space Research V, 546-563, 1965.

Smit, G. J., Oscillatory motion of the nose region of the magnetopause, J. Geophys. Res., 73, 4990-4993, 1968.

Smith, E. J., A comparison of Explorer 6 and Explorer 10 magnetometer data, J. Geophys. Res., 67, 2045-2049, 1962.

Smith, E. J., P. J. Coleman, D. L. Judge and C. P. Sonett, Characteristics of the extraterrestrial current system: Explorer VI and Pioneer V, J. Geophys. Res., 65, 1858-1861, 1960.

Smith, E. J., C. P. Sonett, and J. W. Dungey, Satellite observations of the geomagnetic field during magnetic storms, J. Geophys. Res., 69, 2669-2688, 1964.

Sonett, C. P., E. J. Smith, D. L. Judge, and P.J. Coleman, Current systems in the vestigial geomagnetic field: Explorer 6, Phys. Rev. Letters, 4, 161-163, 1960.

Speiser, T. W., Acceleration of particles in the neutral sheet of the geomagnetic tail, Proc.of the Int'l Conf. on Cosmic Rays, p. 147 London, 1966.

Speiser, T. W. and N. F. Ness, The neutral sheet in the geomagnetic tail: its motion, equivalent currents, and field line connection through it, J. Geophys. Res., 72, 131-142, 1967.

Sugiura, M., T. L. Skillman, B. G. Ledley and J. P. Heppner, Propagation of the sudden commencement of 8 July 1966 to the magnetotail, NASA-GSFC preprint X612-68-235, 1968.

Van Allen, J. A., Absence of 40-kev electrons in the earth's magnetospheric tail at 3300 earth radii, J. Geophys. Res., 70, 4731-4739, 1965.

Van Allen, J. A. and N. F. Ness, Particle shadowing by the moon, U. of Iowa preprint 68-46, 1968.

Wolfe, J. H., R. W. Silva, D. D. McKibbin, and R. H. Mason, Preliminary observations of a geomagnetic wake at 1000 earth radii, J. Geophys. Res., 72, 4577, 1967.

FIGURE CAPTIONS

Figure 1 Ecliptic plane projection of high apogee (> 20 R_E) spacecraft that have provided experimental observations of the geomagnetic tail from 1961-1968. Not shown are the circular orbits of the Vela series, between 15-19 R_E, which obtained significant data on the imbedded plasma sheet or the orbit of Explorer 14, apogee = 15.9 R_E.

Figure 2 Schematic diagram of the spatial distribution of electrons (E_e > 45 kev) obtained by Explorer 14 in 1963 near the noon-midnight geomagnetic meridian plane (Frank, 1964).

Figure 3 A composite of selected magnetic field observations by Explorer 14 projected into a local geomagnetic meridian plane. The shaded area shows the range of geomagnetic latitudes of the anti-solar direction in the midnight meridian plane (Cahill, 1966).

Figure 4 Schematic diagrams of two theories of the geomagnetic tail, circa 1965. The upper version is based upon magnetic merging at a neutral line while the lower figure assumes no merging.

Figure 5 Magnetic field measurements of the geomagnetic tail near the midnight meridian plane by IMP 1. The field direction closely parallels the earth-sun line with a rapid change from antisolar to solar directed sense while inbound at a radial distance of 16 R_E (Ness, 1965). Dashed lines represent the theoretical geomagnetic field.

Figure 6 Interpretation of IMP 1 geomagnetic tail field (vectors) and neutral sheet crossings (dots) within 2 R_E of the noon-midnight meridian plane in solar magnetospheric coordinates.

χ_{SS} represents the geomagnetic latitude of the subsolar point, the "angle of attack" of the solar wind flow (Speiser and Ness, 1966).

Figure 7 Simultaneous electron flux ($E_e > 45$ kev) and magnetic field measurements by IMP 1 in 1964 showing decreased field magnitudes across multiple plasma sheet crossings between 25-27 R_E and 24 hours later between 17-18 R_E. Note correlated field decreases and flux increases, Anderson's electron islands, throughout this inbound pass (Anderson and Ness, 1966).

Figure 8 Simultaneous measurements of the geomagnetic tail by IMP 1 and the boundary of trapped radiation by the satellite 1963-38C (+) during a geomagnetic storm in 1964. The invariant latitude, , is theoretically predicted using the observed field magnitude, which is seen to be positively correlated with Kp (Ness and Williams, 1966).

Figure 9 Projection of hourly average magnetic field measurements obtained by IMP 2 on the equatorial plane (lower figure) and on four curved meridian planes (upper figure). This illustrates the formation of the geomagnetic tail by the streaming solar wind (Fairfield and Ness, 1967).

Figure 10 Summary of Explorer 33 bow shock and magnetopause traversals, rotated into the ecliptic plane assuming cylindrical symmetry about the earth-sun line (Behannon, 1967).

Figure 11 Representative magnetic field data in the geomagnetic tail obtained by Explorer 33 on September 14, 1966 (upper figure) and October 21, 1966 (lower figure). Position of satellite in solar ecliptic coordinates is given at bottom (Behannon 1967).

Figure 12 Average vector magnetic field observed in the geomagnetic tail by Explorer 33 during July-November 1966. The uppermost figure represents the projection on the noon-midnight plane in solar magnetosphere coordinates. The lower two figures represent separate projections on the equatorial plane for data obtained either above or below the plane $Z_{SM}=3\ R_E$ (Behannon, 1967).

Figure 13 Distribution of undisturbed hourly average magnetic tail field magnitudes as a function of distance obtained by Explorer 33 during July-November, 1966. Data points circled represent large increases followed one hour later by a corresponding increase in Kp (Behannon, 1967).

Figure 14 Spectrums of electron counting rates measured in the magnetosheath and the plasma sheet by the Vela satellites (Bame et al., 1967).

Figure 15 Measurements of the electron component of the plasma sheet by Vela 2B showing the absence of the electron population ($Ee > 350$ kev) while crossing the sheet. The arrows indicate that the flux was less than detector background level (Bame et al., 1967). See Figure 16.

Figure 16 Differential electron energy spectrums obtained at lettered

times in Figure 15. The negative exponent values for the power-law high-energy tail are given shown (Bame et al.,1967).

Figure 17 Interpretation of the configuration of the plasma sheet in the geomagnetic tail for χ_{ss}= +12°. The actual range of positions of the plasma sheet determined from the Vela measurements is indicated at 17 R_E (Bame et al., 1967).

Figure 18 Pioneer 7 trajectory (solid line) in the Y_{sm}-Z_{sm} plane. The shaded portions represent intervals with significant electron fluxes. The dotted curve gives the predicted neutral sheet position using the model shown in the insert (Lazarus et al., 1968).

Figure 19 Measurements of the magnetic field intensity and electron velocity and density by Pioneer 7 in 1966. Vertical bars and dots indicate ranges of uncertainty of the plasma parameters assuming different spectral shapes. Gaps in plasma data indicate fluxes less than detector threshold. The field decrease from 0100 to 0130 represents traversal of the neutral sheet (Lazarus et al., 1968).

Figure 20 Detailed magnetic field measurements and RMS deviations obtained by Pioneer 7 in 1966 showing increase in fluctuations as field reversal region is tranversed.

Figure 21 Ecliptic plane projections of the trajectories of Pioneers 7 and 8 showing passage through the geomagnetospheric tail and wake regions at 1000 R_E and 500 R_E respectively in 1966 and 1968.

Figure 22 Detailed magnetic field measurements of anti-solar directed field lines by Pioneer 7 assumed to be extended from the Earth to 1000 R_E. An indication of anomalous plasma conditions observed by the MIT group on the same spacecraft is indicated.

Figure 23 Schematic diagrams of the geomagnetic field and tail formed by the solar wind. Compare the lower diagram with that in Figure 4 showing a change from no merging across the neutral section in the tail to merging occuring relatively close to the earth.

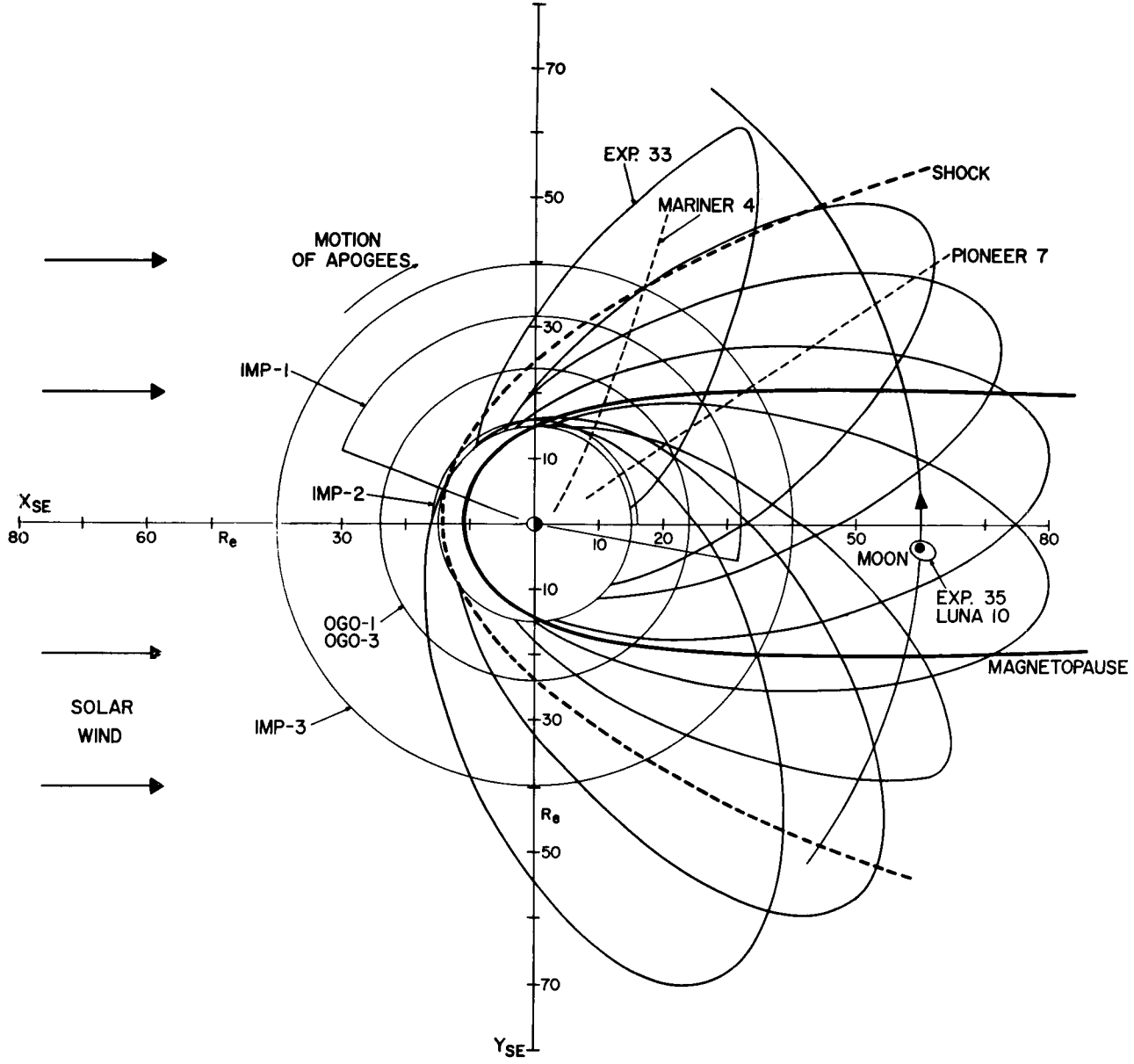
70
50
30
10
10
30
50
70
EXP. 33
MARINER 4
SHOCK
PIONEER 7
MOTION
OF APOGEES
IMP-1
IMP-2
IMP-3
OGO-1
OGO-3
X_{SE}
80
60
R_e
30
10
20
50
80
MOON
EXP. 35
LUNA 10
MAGNETOPAUSE
SOLAR
WIND
R_e
Y_{SE}

FIGURE 1

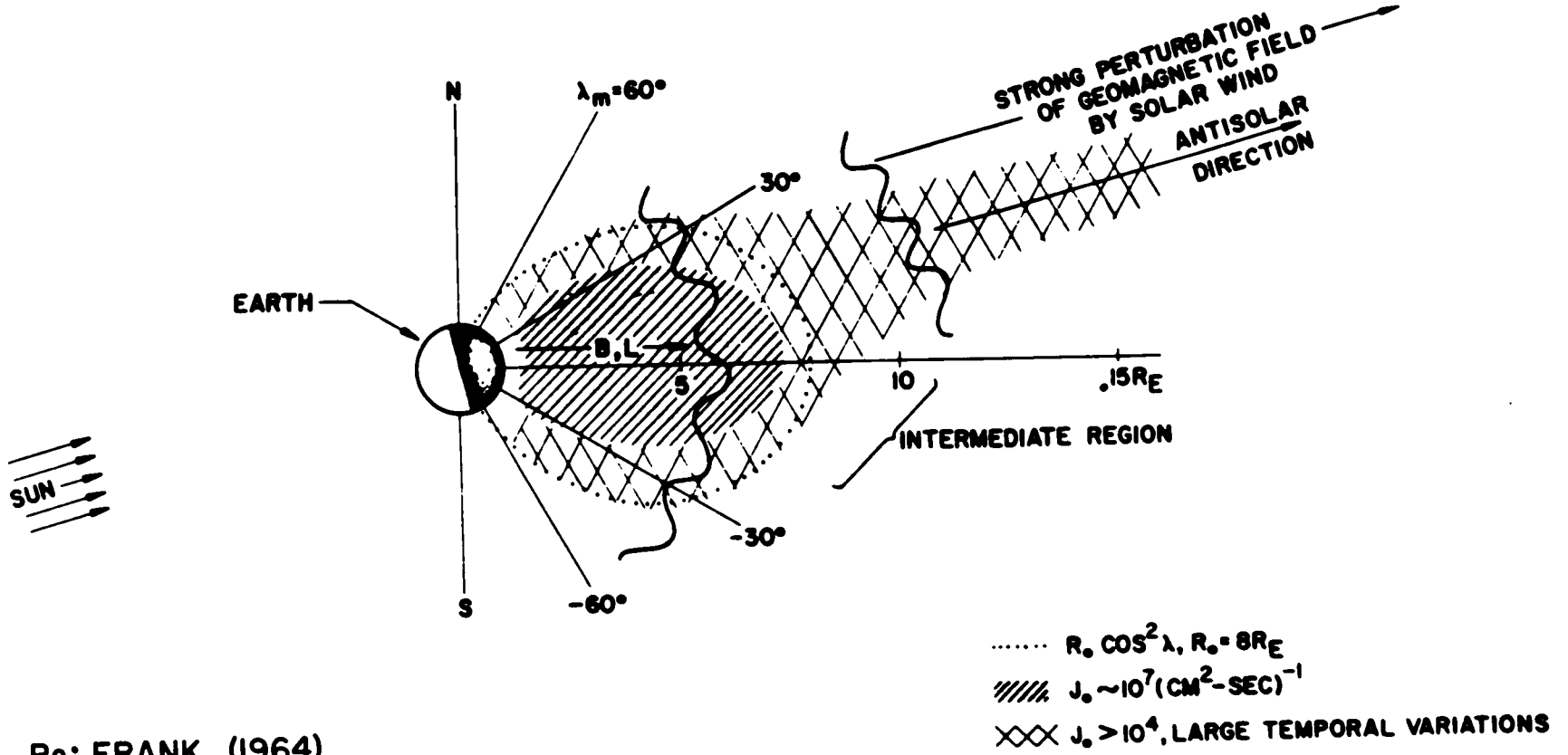

Re: FRANK (1964)

FIGURE 2

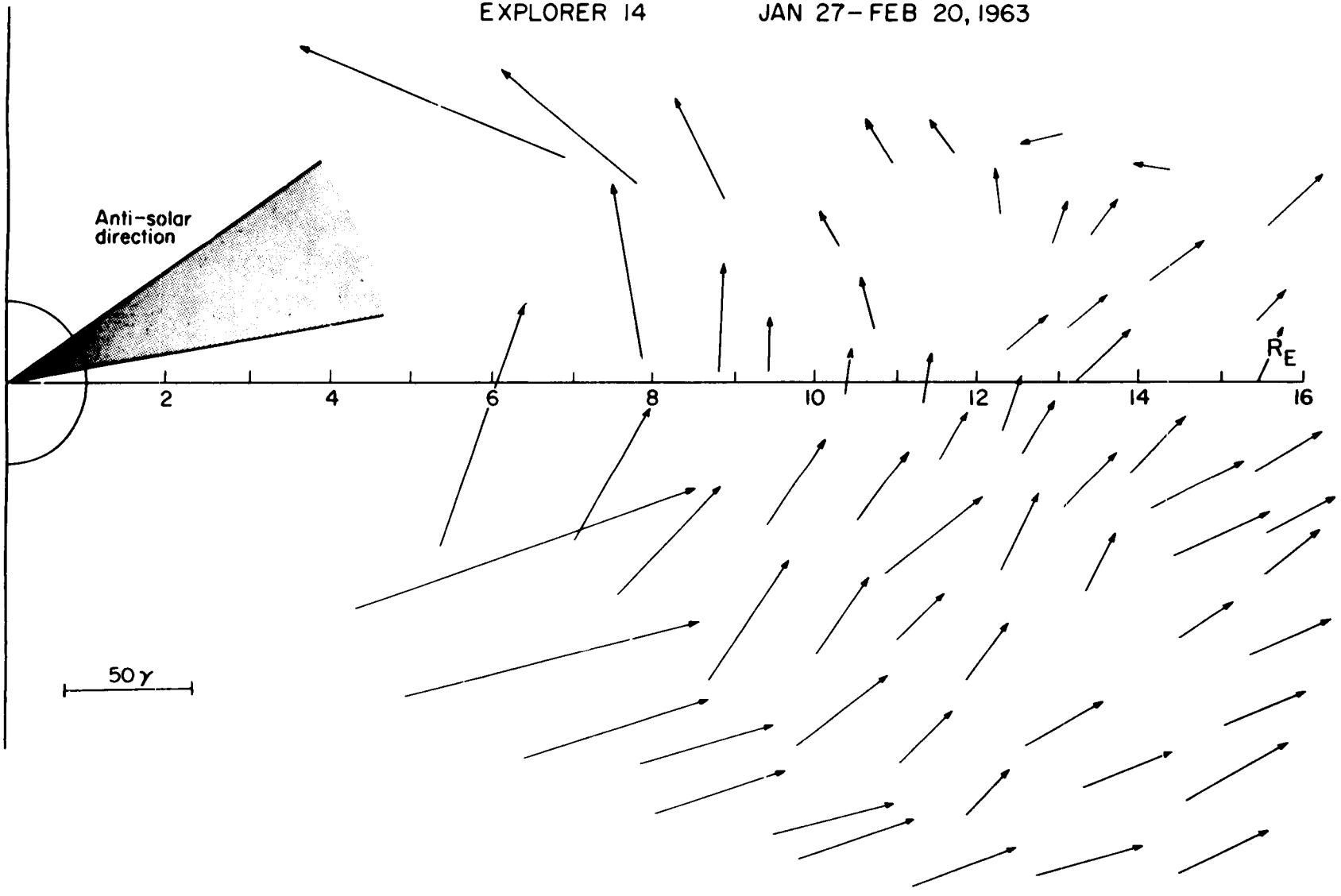
EXPLORER 14
JAN 27-FEB 20, 1963
Anti-solar direction
2
4
6
8
10
12
14
16
R_E
50γ

FIGURE 3

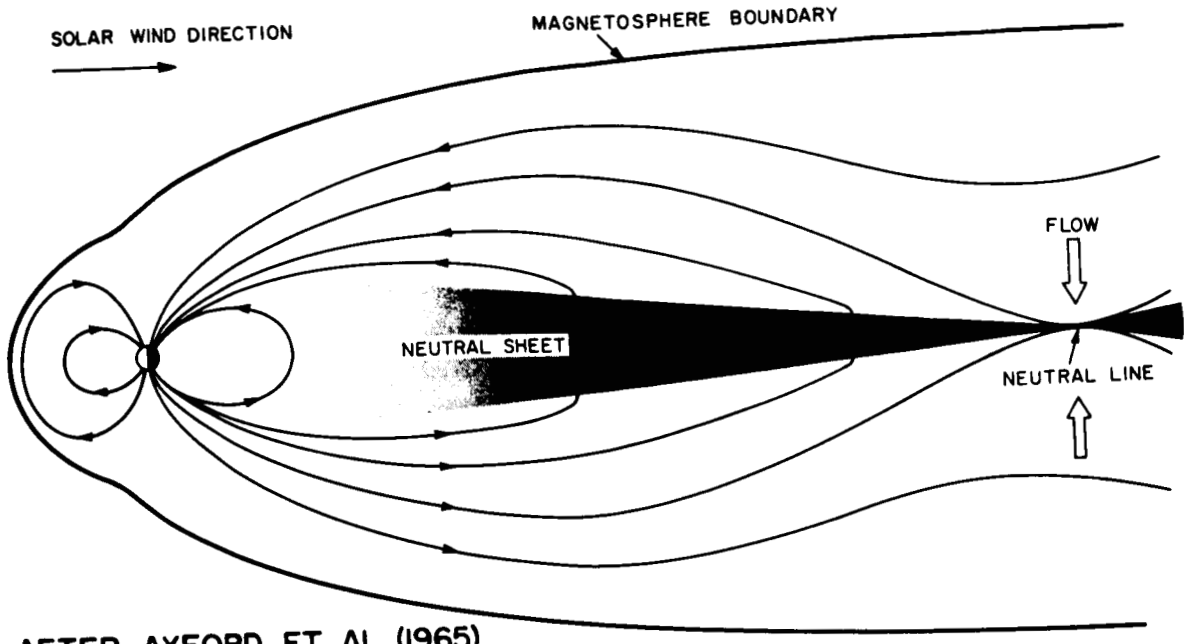

AFTER AXFORD ET. AL. (1965)

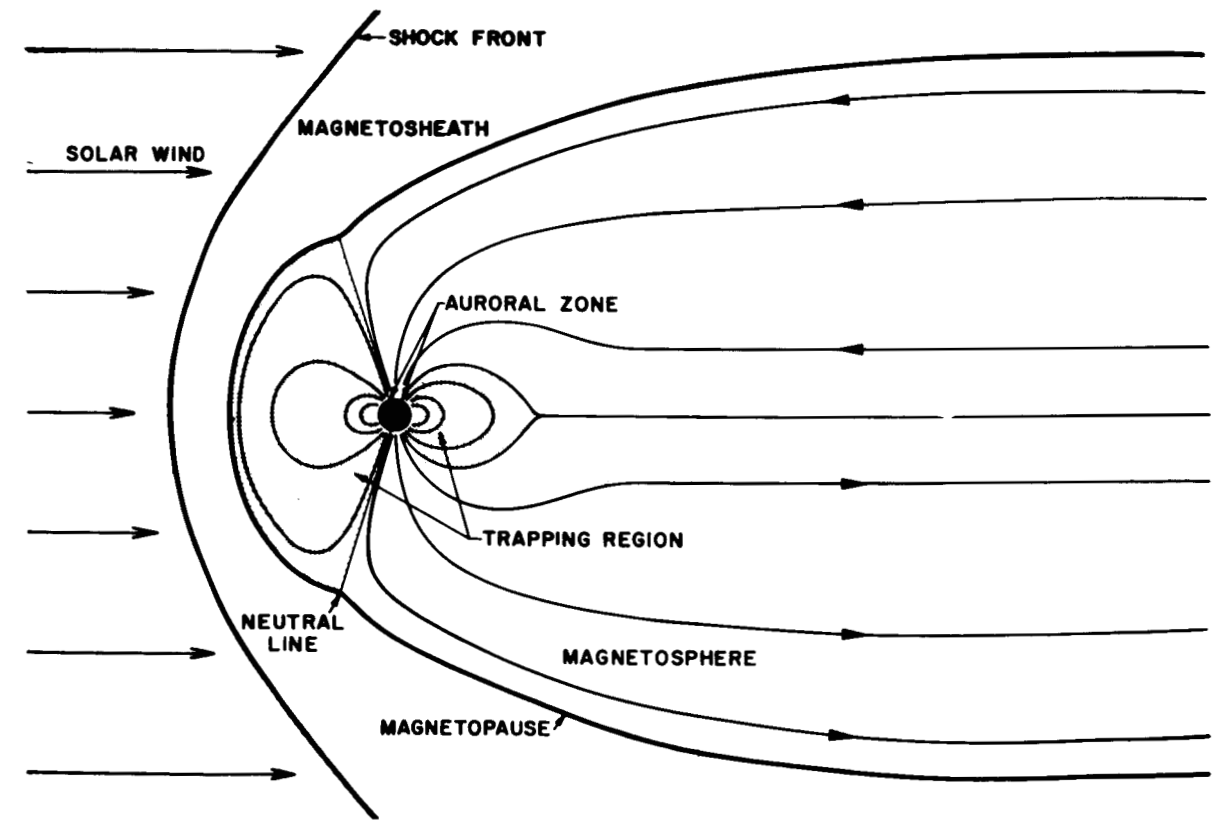

AFTER DESSLER & JUDAY (1965)

FIGURE 4

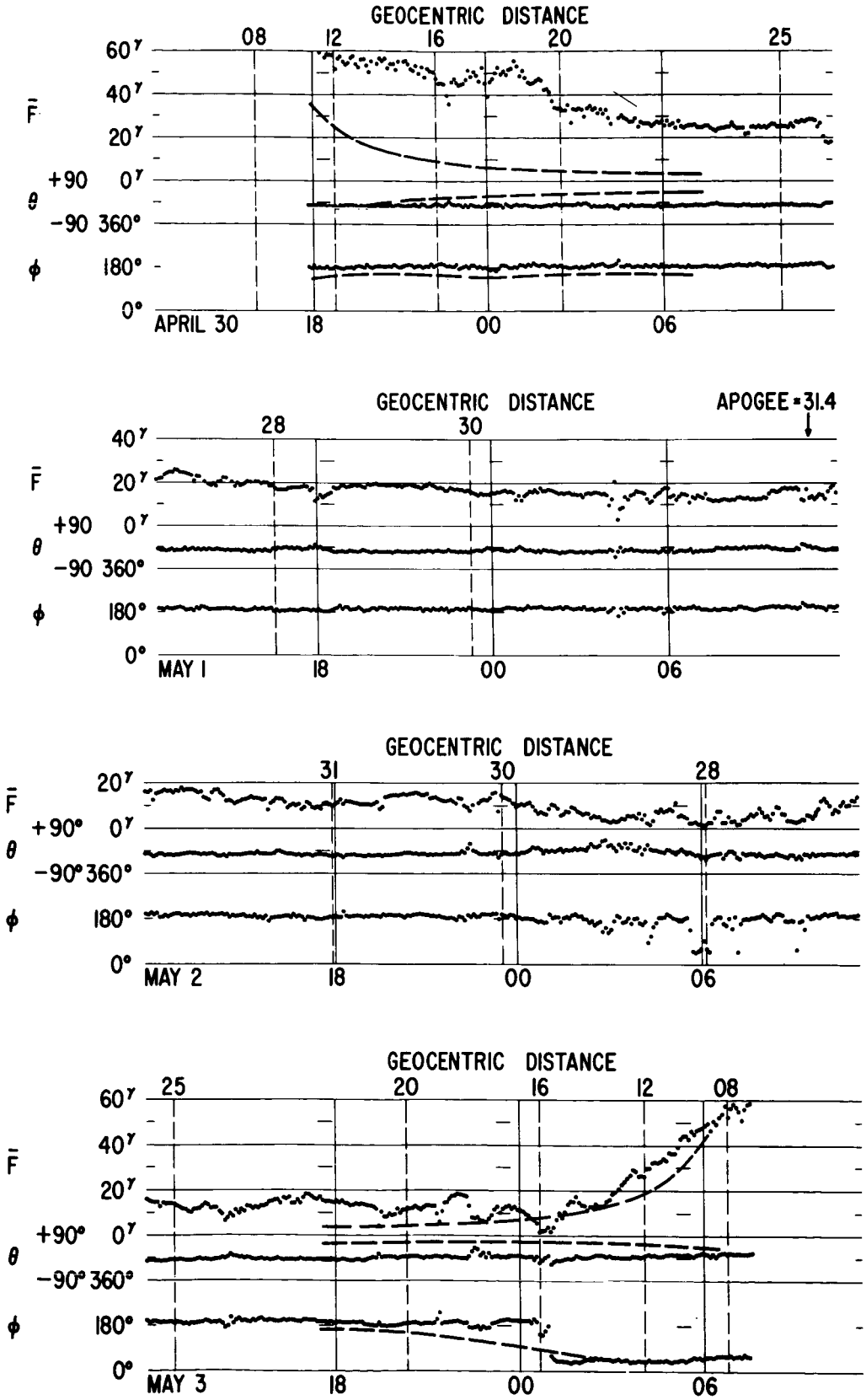

ORBIT NO. 41 IMP-I 1964

FIGURE 5

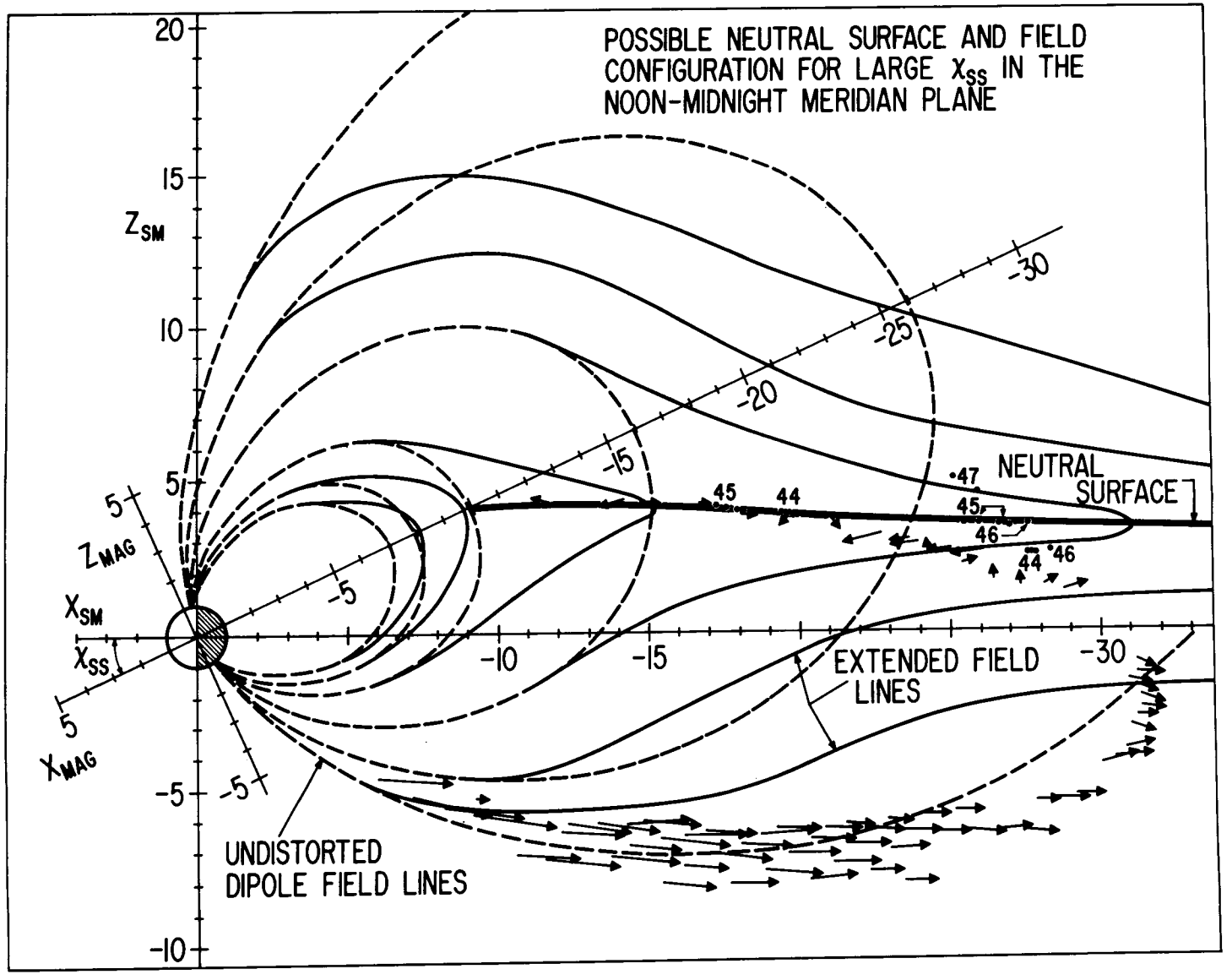
POSSIBLE NEUTRAL SURFACE AND FIELD CONFIGURATION FOR LARGE χ_{ss} IN THE NOON-MIDNIGHT MERIDIAN PLANE
Z_{SM}
Z_{MAG}
X_{SM}
χ_{ss}
X_{MAG}
NEUTRAL SURFACE
EXTENDED FIELD LINES
UNDISTORTED DIPOLE FIELD LINES
20
15
10
5
-5
-10
-30
-25
-20
-15
-10
-5
45
44
47
46

FIGURE 6

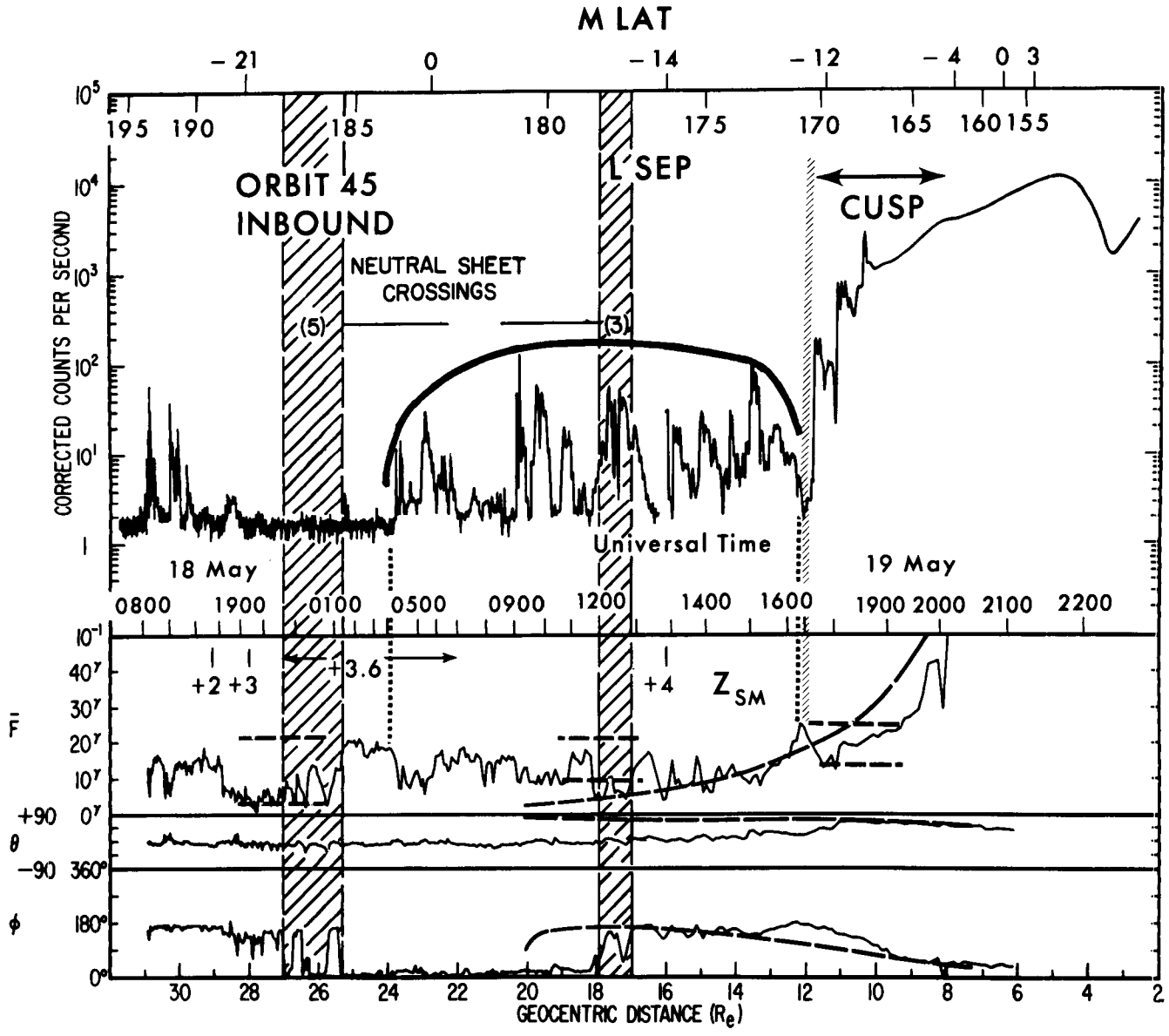
M LAT
- 21
0
- 14
- 12
- 4
0
3
195
190
185
180
175
170
165
160
155
ORBIT 45
INBOUND
L'SEP
CUSP
NEUTRAL SHEET
CROSSINGS
(5)
(3)
CORRECTED COUNTS PER SECOND
Universal Time
18 May
19 May
0800
1900
0100
0500
0900
1200
1400
1600
1900
2000
2100
2200
+2
+3
+3.6
+4
Z_{SM}
F
θ
φ
+90
-90
360°
180°
0°
30
28
26
24
22
20
18
16
14
12
10
8
6
4
2
GEOCENTRIC DISTANCE (R_e)

FIGURE 7

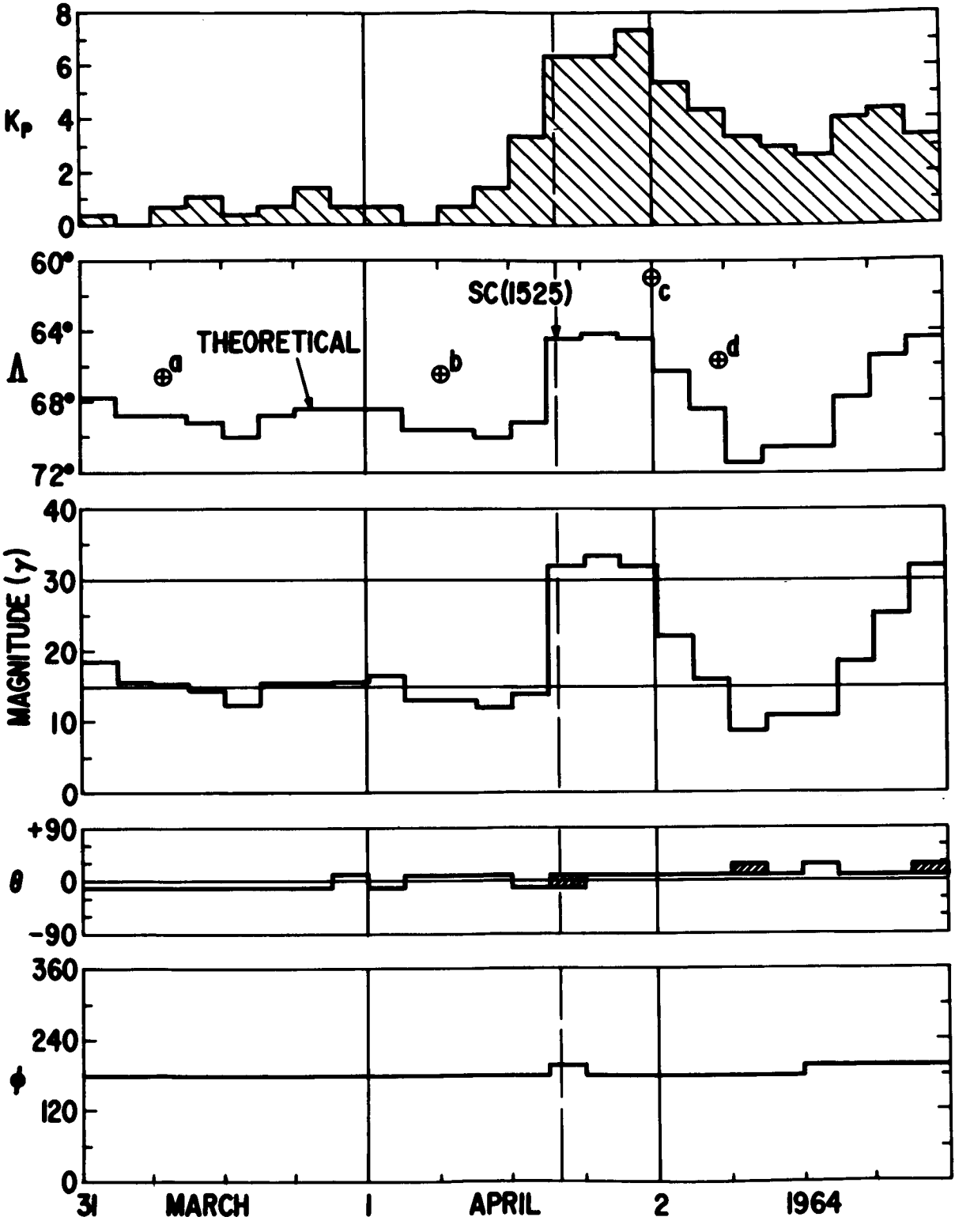
8
6
4
2
0
K_p
60°
64°
68°
72°
Λ
THEORETICAL
SC(1525)
⊕a
⊕b
⊕c
⊕d
40
30
20
10
0
MAGNITUDE (γ)
+90
0
-90
θ
360
240
120
0
φ
31
MARCH
1
APRIL
2
1964

FIGURE 8

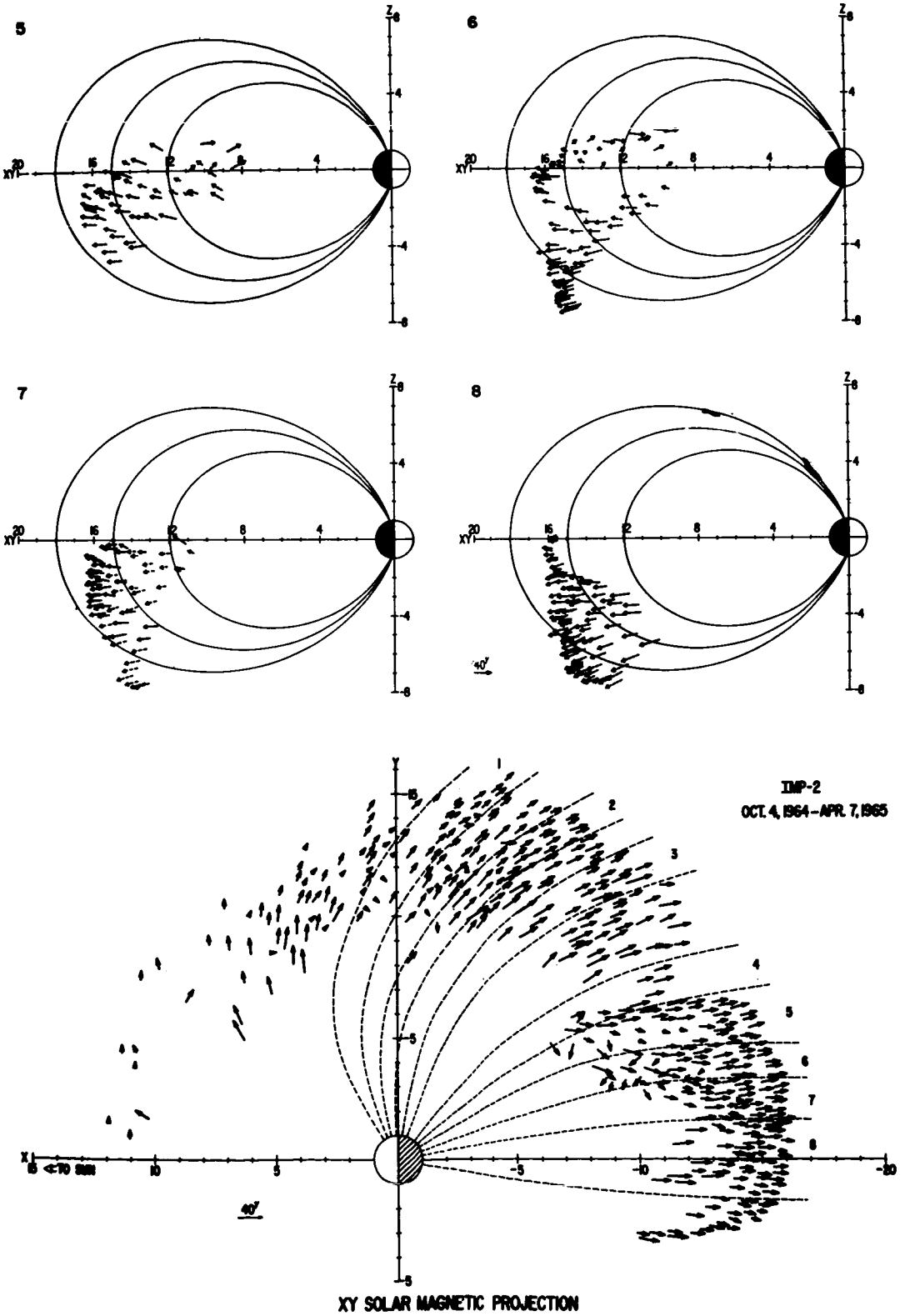

FIGURE 9

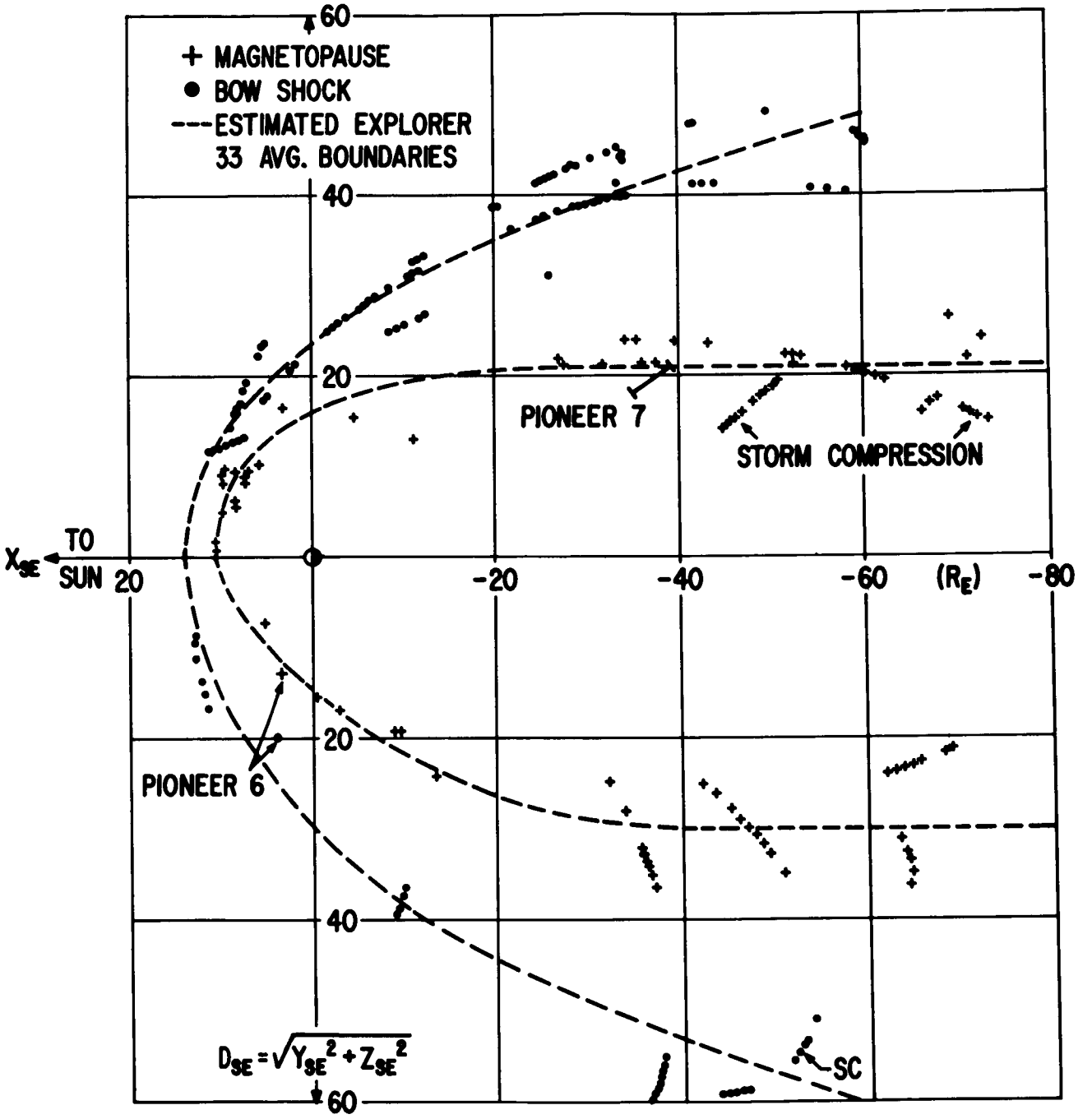
+ MAGNETOPAUSE
● BOW SHOCK
---ESTIMATED EXPLORER 33 AVG. BOUNDARIES
60
40
20
PIONEER 7
STORM COMPRESSION
TO SUN
X_{SE}
20
-20
-40
-60
(R_E)
-80
20
PIONEER 6
40
$D_{SE} = \sqrt{Y_{SE}^2 + Z_{SE}^2}$
SC
60

FIGURE 10

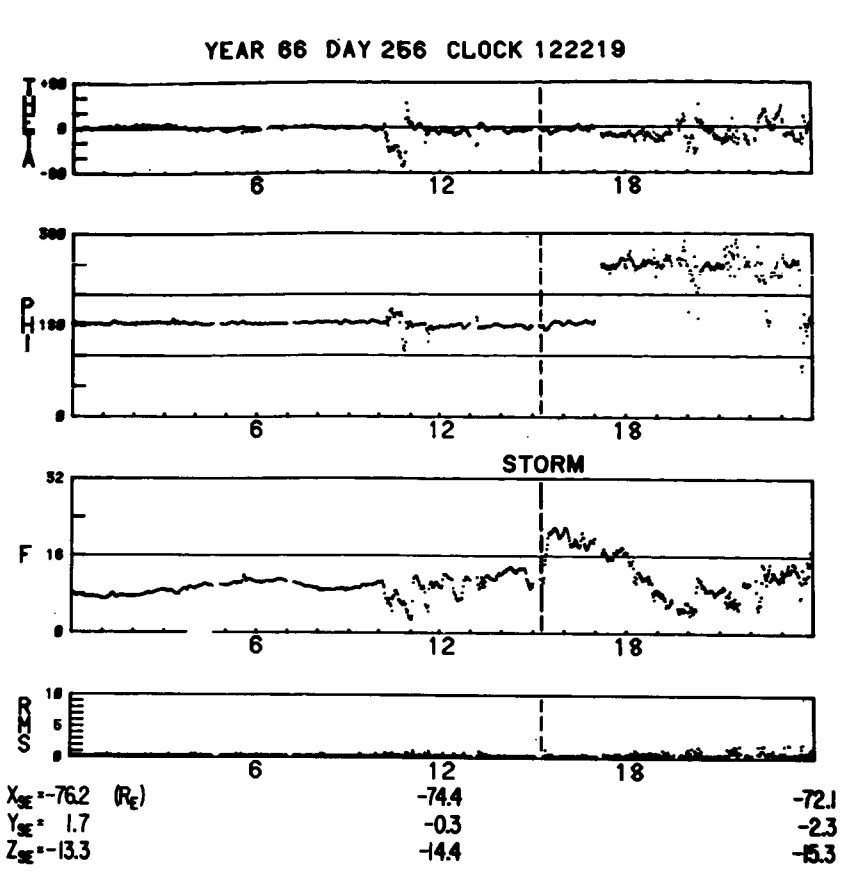
YEAR 66 DAY 256 CLOCK 122219
THETA
PHI
STORM
F
RMS
6
12
18
X_{SE}=-76.2 (R_E) -74.4 -72.1
Y_{SE}= 1.7 -0.3 -2.3
Z_{SE}=-13.3 -14.4 -15.3

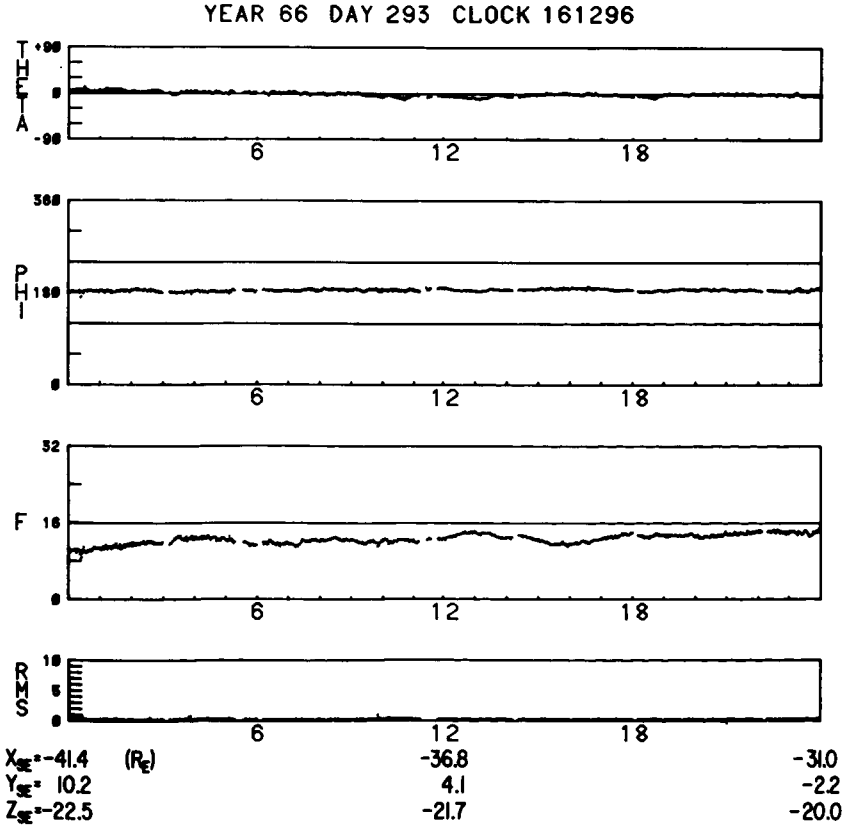
YEAR 66 DAY 293 CLOCK 161296
THETA
PHI
F
RMS
6
12
18
X_{SE}=-41.4 (R_E) -36.8 -31.0
Y_{SE}= 10.2 4.1 -2.2
Z_{SE}=-22.5 -21.7 -20.0

FIGURE 11

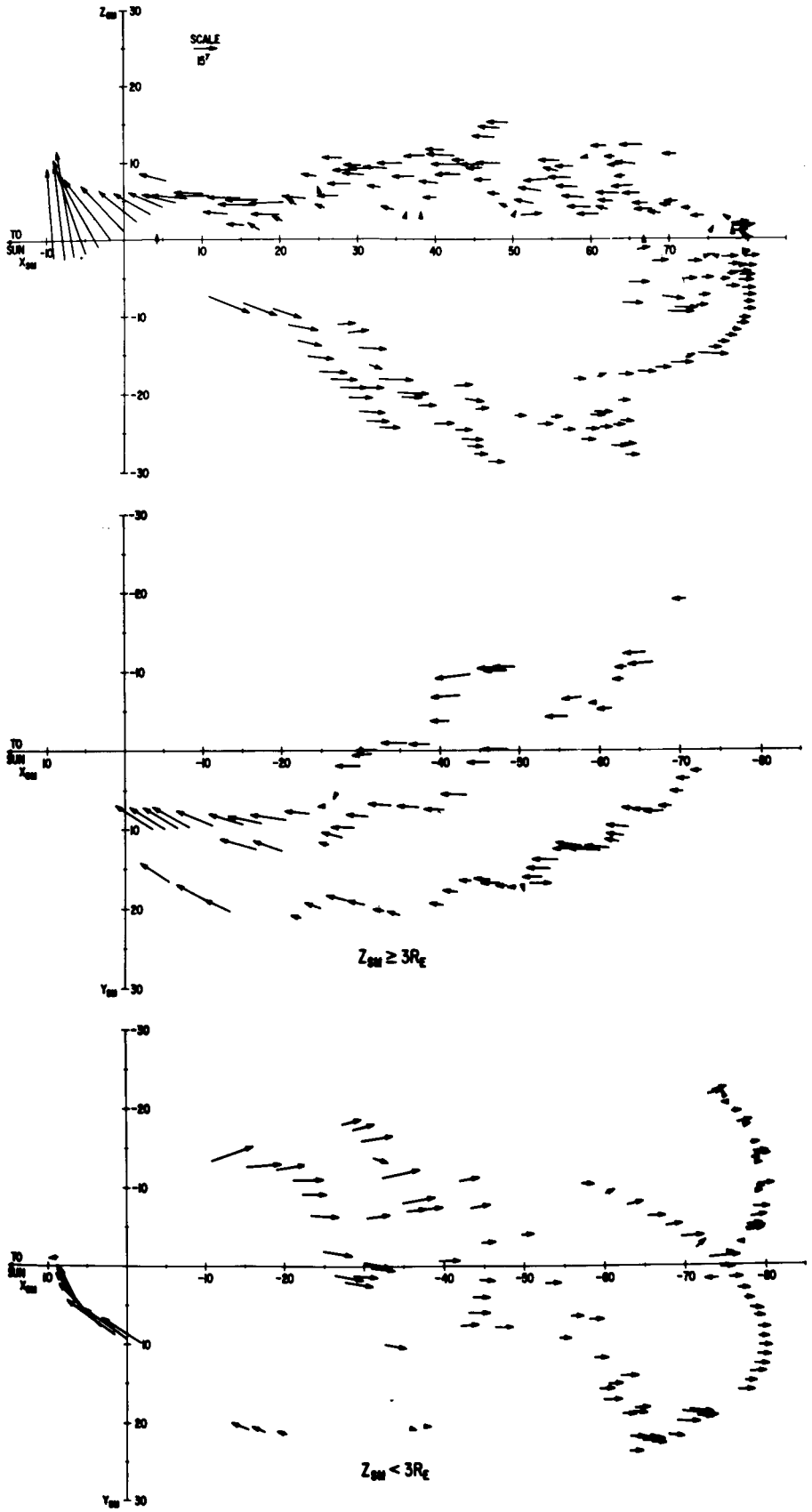

FIGURE 12

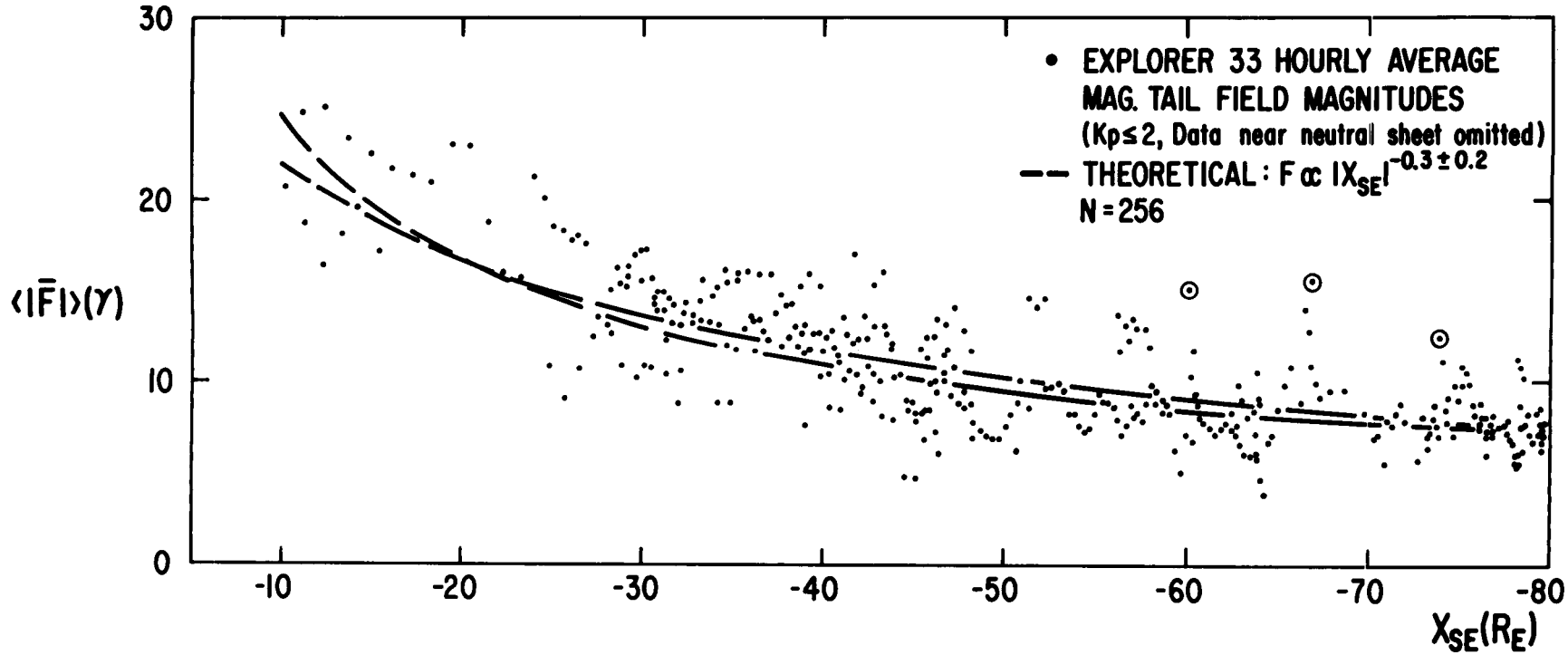
30
20
10
0
-10
-20
-30
-40
-50
-60
-70
-80
$\langle|\bar{F}|\rangle(\gamma)$
$X_{SE}(R_E)$
• EXPLORER 33 HOURLY AVERAGE
MAG. TAIL FIELD MAGNITUDES
(Kp≤2, Data near neutral sheet omitted)
— THEORETICAL : $F \propto |X_{SE}|^{-0.3 \pm 0.2}$
N = 256

FIGURE 13

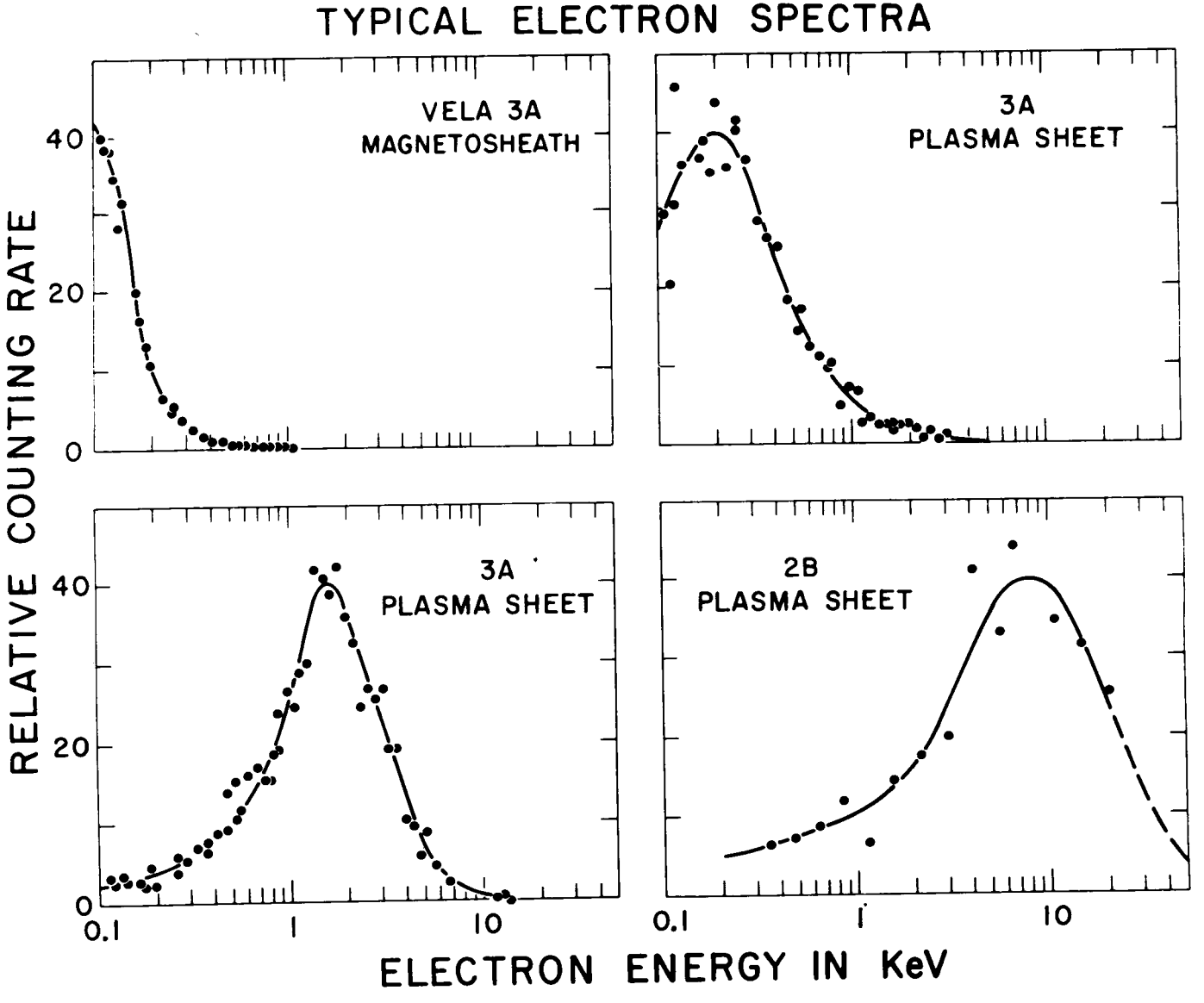
TYPICAL ELECTRON SPECTRA
VELA 3A
MAGNETOSHEATH
3A
PLASMA SHEET
3A
PLASMA SHEET
2B
PLASMA SHEET
RELATIVE COUNTING RATE
0
20
40
0.1
1
10
ELECTRON ENERGY IN KeV

FIGURE 14

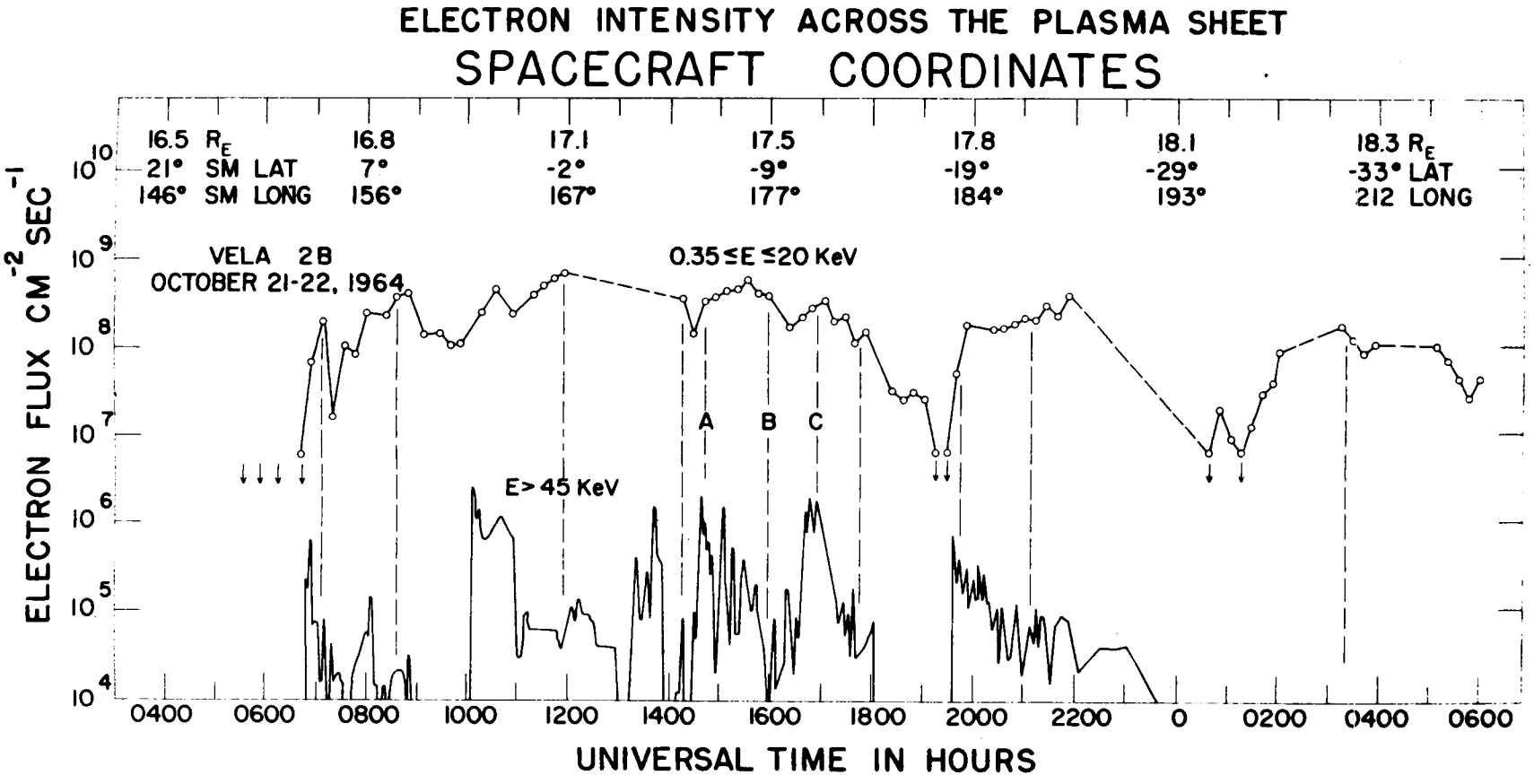
ELECTRON INTENSITY ACROSS THE PLASMA SHEET
SPACECRAFT COORDINATES
16.5 R_E
21° SM LAT
146° SM LONG
16.8
7°
156°
17.1
-2°
167°
17.5
-9°
177°
17.8
-19°
184°
18.1
-29°
193°
18.3 R_E
-33° LAT
212 LONG
VELA 2B
OCTOBER 21-22, 1964
0.35≤E≤20 KeV
E>45 KeV
A
B
C
ELECTRON FLUX CM^{-2} SEC^{-1}
10^{10}
10^{9}
10^{8}
10^{7}
10^{6}
10^{5}
10^{4}
0400
0600
0800
1000
1200
1400
1600
1800
2000
2200
0
0200
0400
0600
UNIVERSAL TIME IN HOURS

FIGURE 15

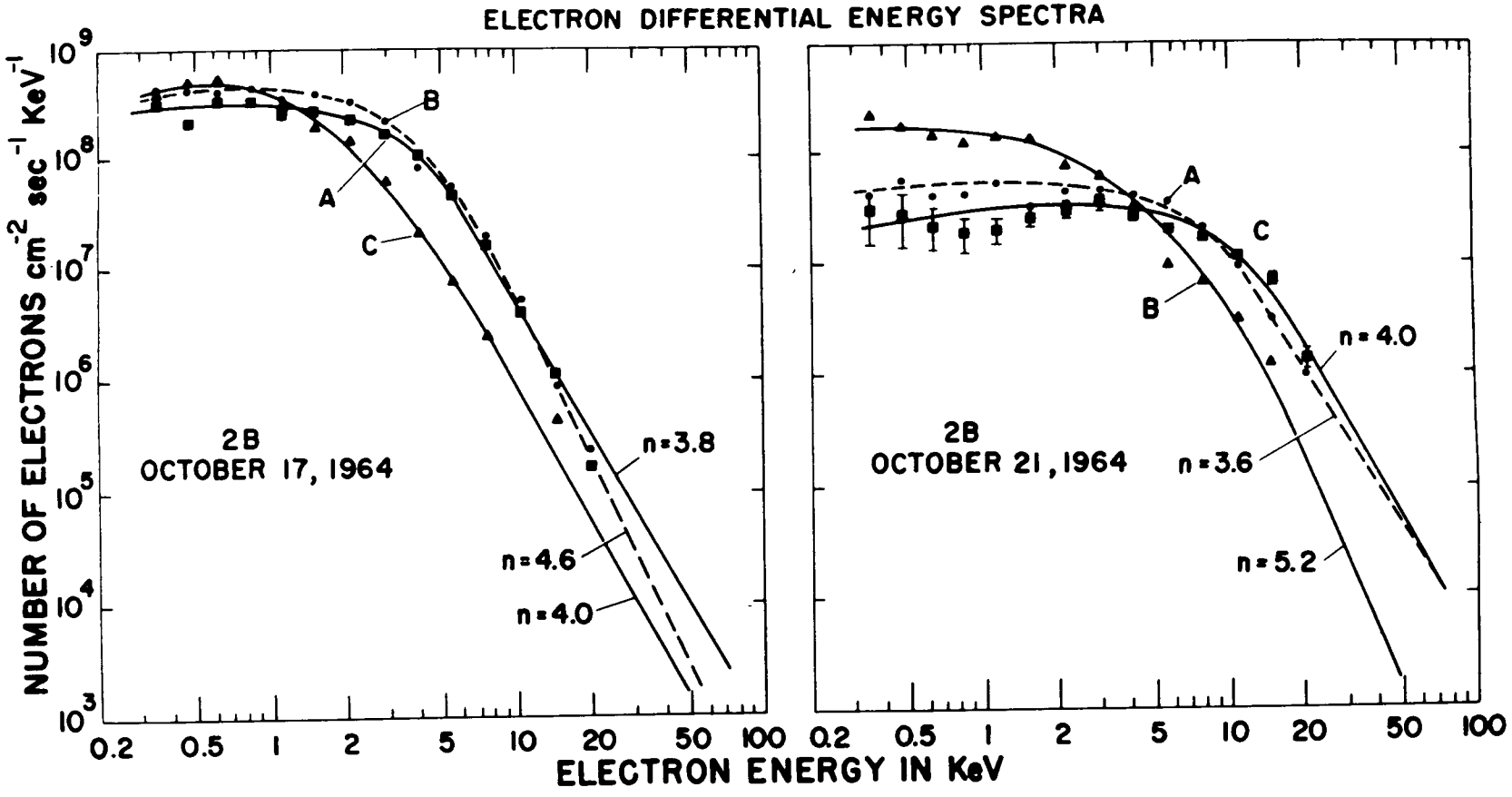
ELECTRON DIFFERENTIAL ENERGY SPECTRA
NUMBER OF ELECTRONS cm⁻² sec⁻¹ KeV⁻¹
ELECTRON ENERGY IN KeV
2B
OCTOBER 17, 1964
A
B
C
n=3.8
n=4.6
n=4.0
2B
OCTOBER 21, 1964
A
B
C
n=4.0
n=3.6
n=5.2

FIGURE 16

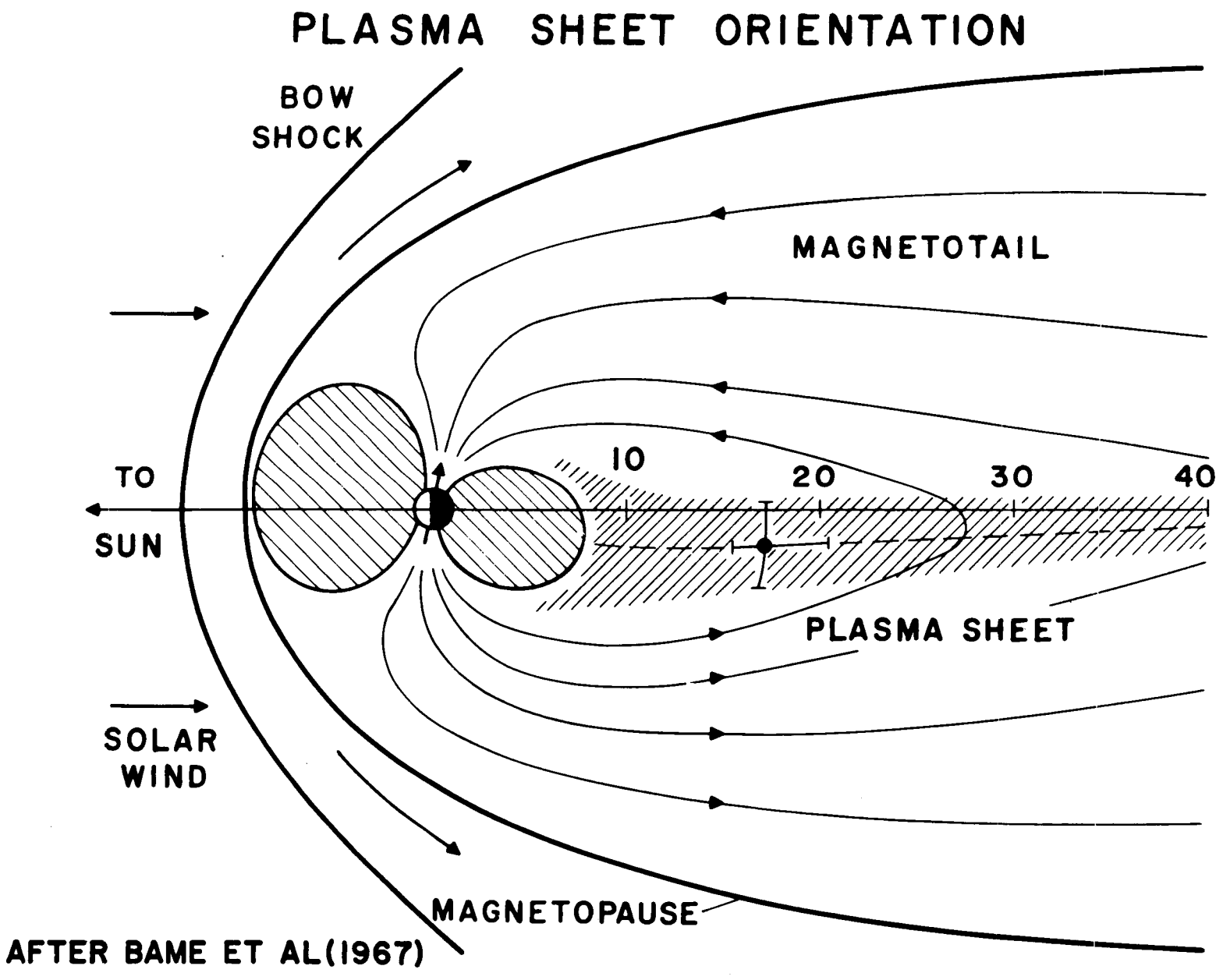
PLASMA SHEET ORIENTATION
BOW SHOCK
MAGNETOTAIL
TO SUN
10
20
30
40
PLASMA SHEET
SOLAR WIND
MAGNETOPAUSE
AFTER BAME ET AL(1967)

FIGURE 17

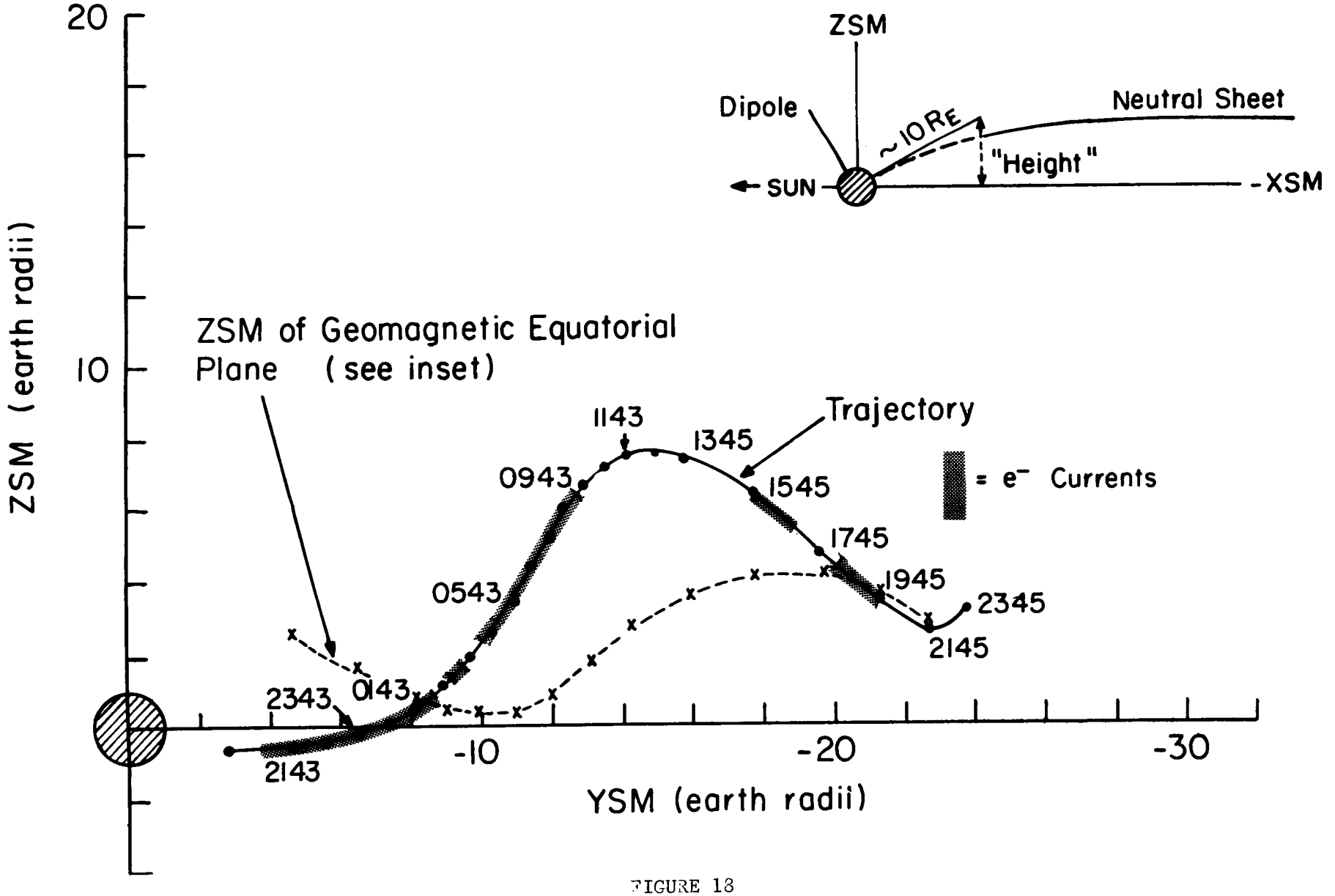
ZSM
Dipole
~10RE
Neutral Sheet
"Height"
SUN
-XSM
20
10
ZSM (earth radii)
ZSM of Geomagnetic Equatorial Plane (see inset)
Trajectory
= e⁻ Currents
1143
1345
0943
1545
1745
1945
2345
2145
0543
0143
2343
2143
-10
-20
-30
YSM (earth radii)

FIGURE 18

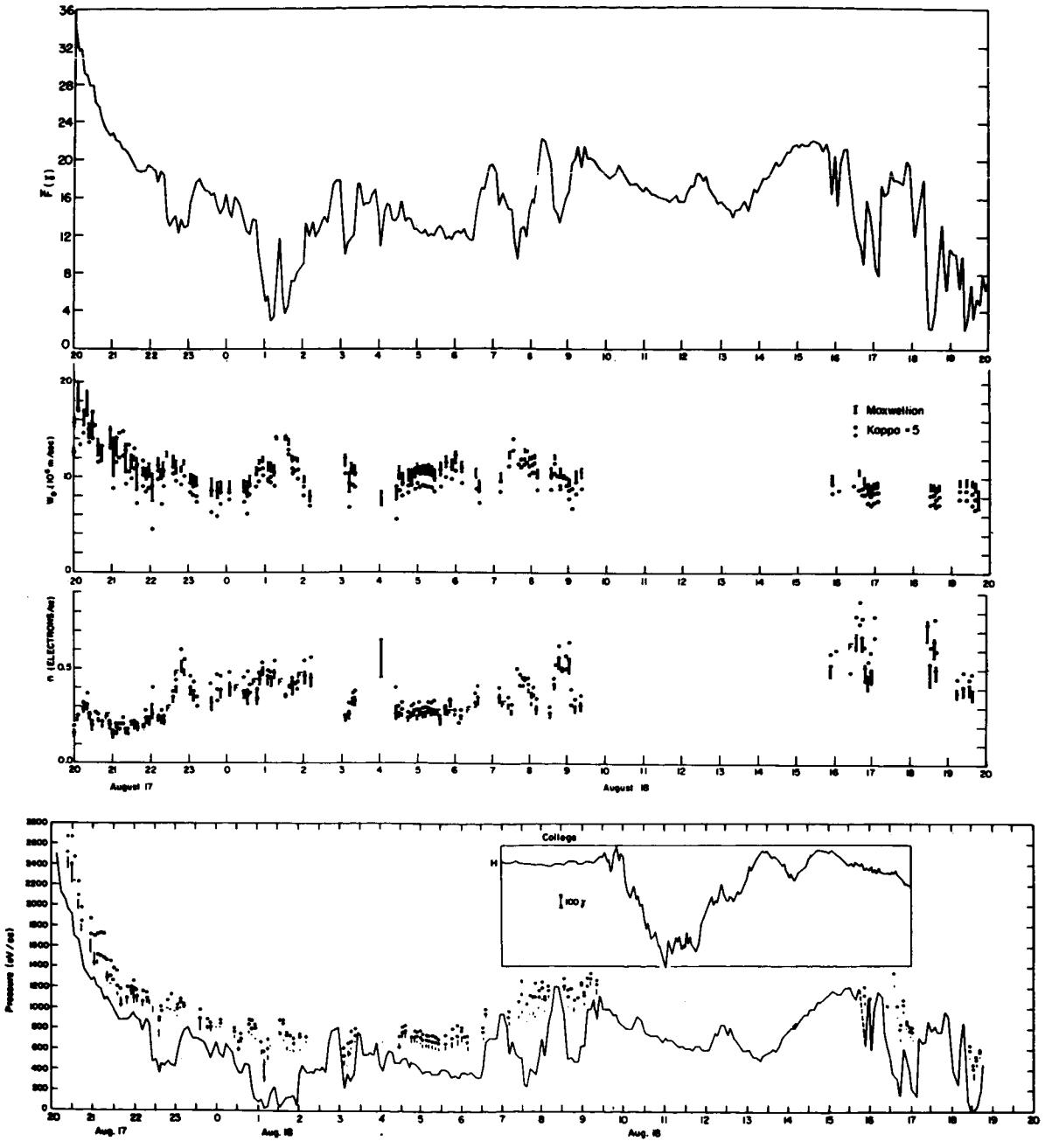
F(t)
Maxwellian
Kappa =5
August 17
August 18
College
H
100 γ
Aug. 17
Aug. 18
Aug. 18

FIGURE 19

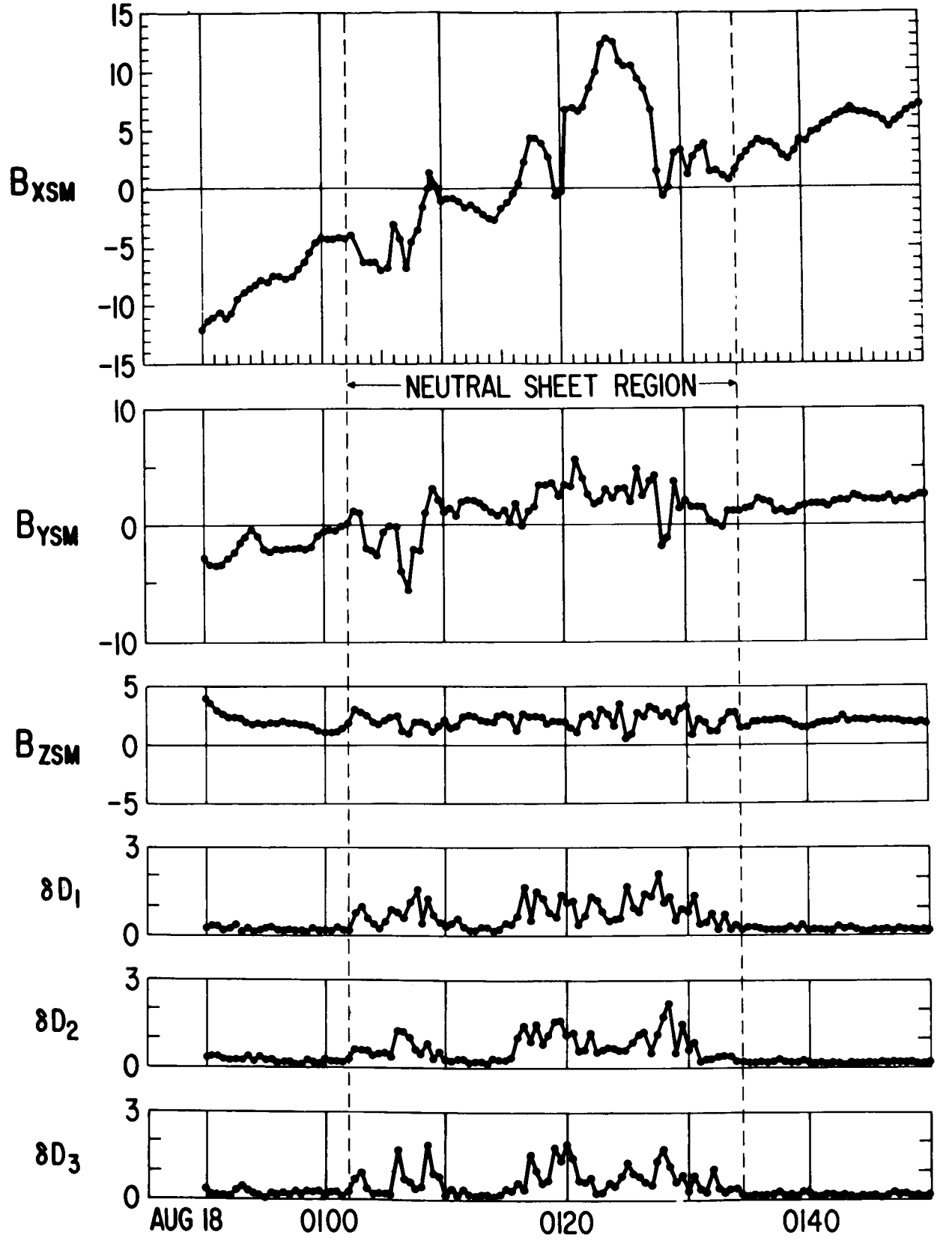
15
10
5
0
-5
-10
-15
B_{XSM}
NEUTRAL SHEET REGION
10
0
-10
B_{YSM}
5
0
-5
B_{ZSM}
3
0
δD_1
3
0
δD_2
3
0
δD_3
AUG 18
0100
0120
0140

FIGURE 20

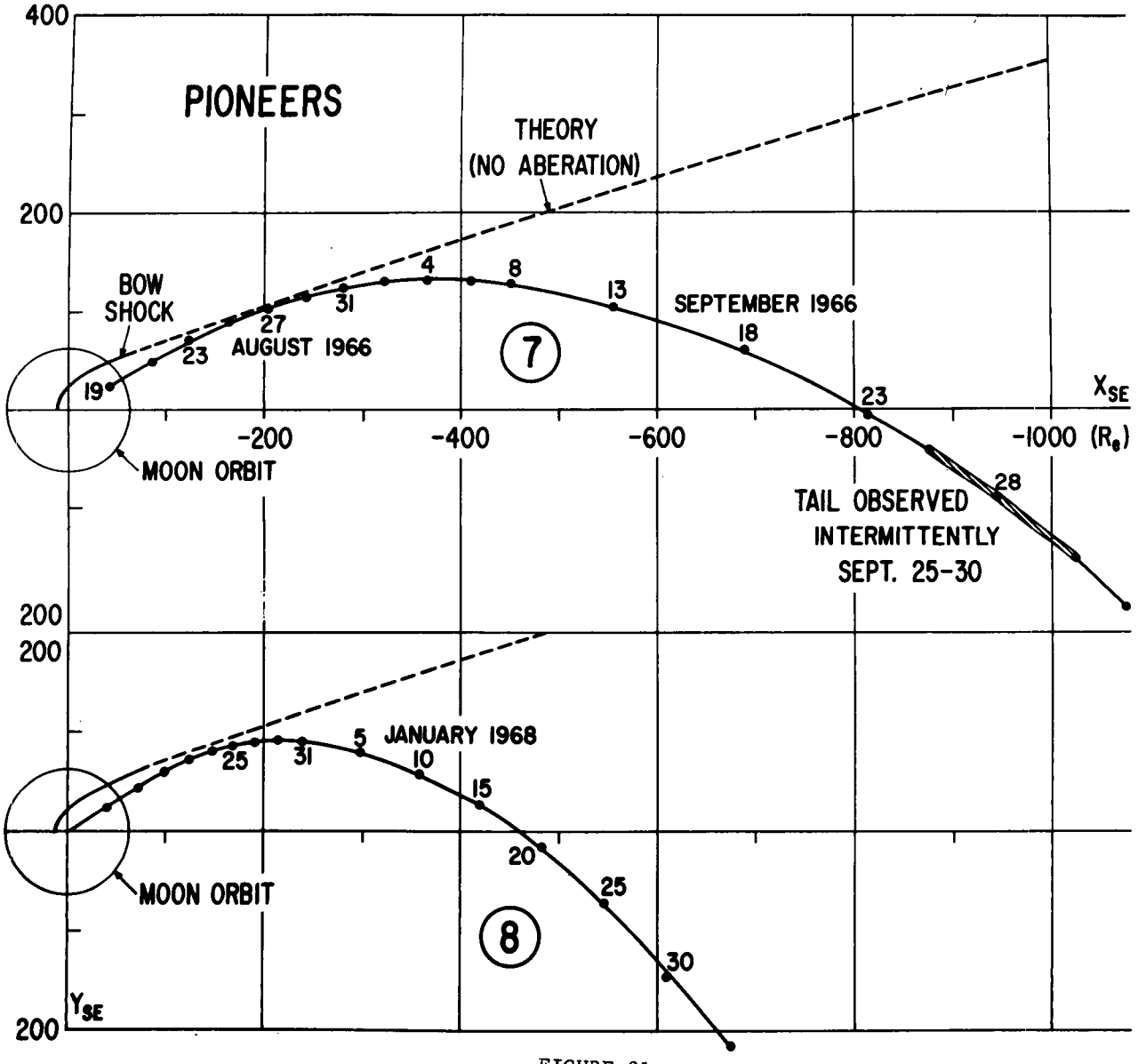
400
PIONEERS
THEORY
(NO ABERATION)
200
BOW
SHOCK
4
8
13
SEPTEMBER 1966
18
27
31
AUGUST 1966
23
19
7
23
X_{SE}
-200
-400
-600
-800
-1000 (R_e)
MOON ORBIT
28
TAIL OBSERVED
INTERMITTENTLY
SEPT. 25-30
200
200
JANUARY 1968
5
25
31
10
15
20
25
MOON ORBIT
8
30
Y_{SE}
200

FIGURE 21

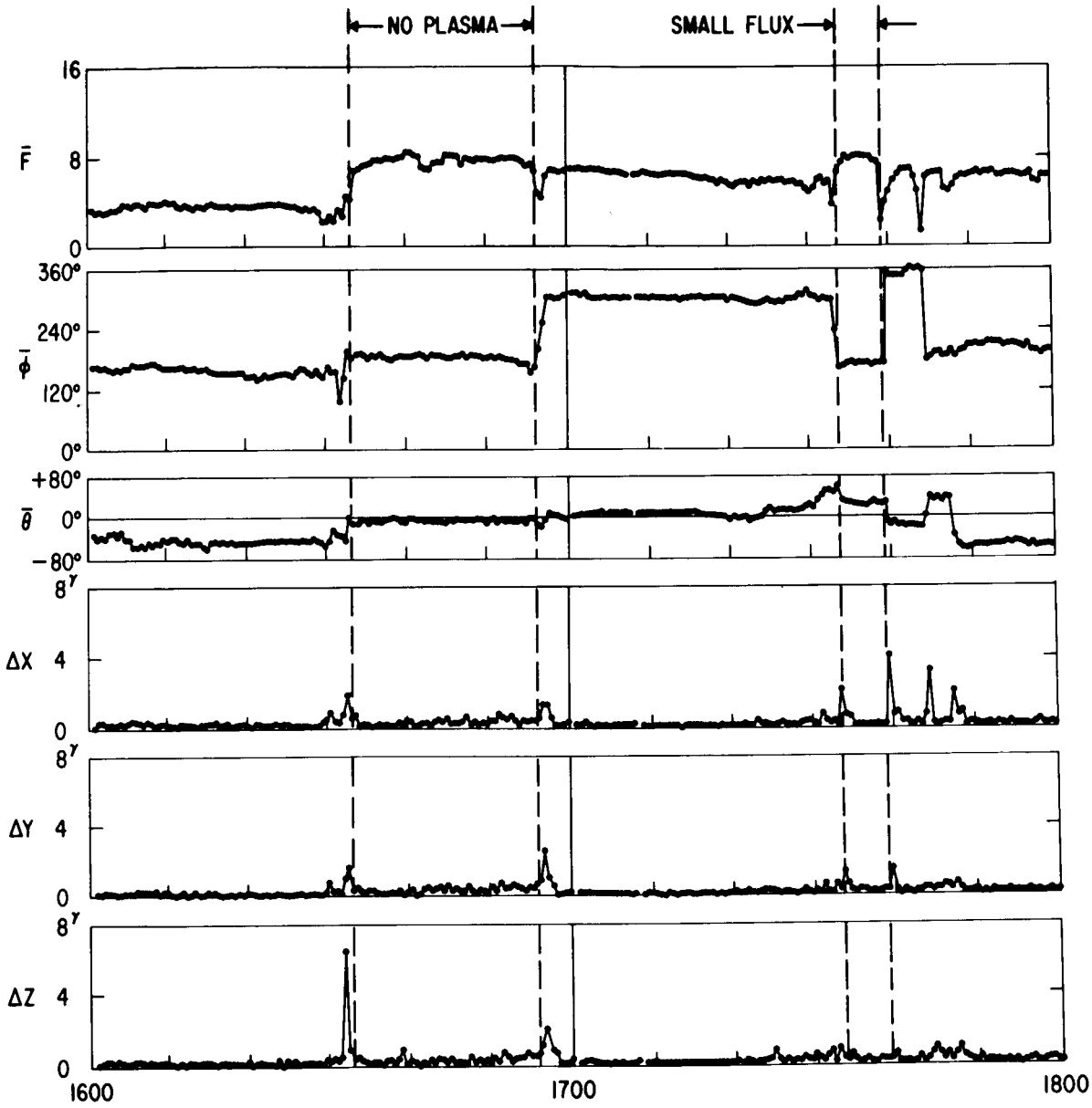

PIONEER 7 SEPT. 26, 1966

FIGURE 22

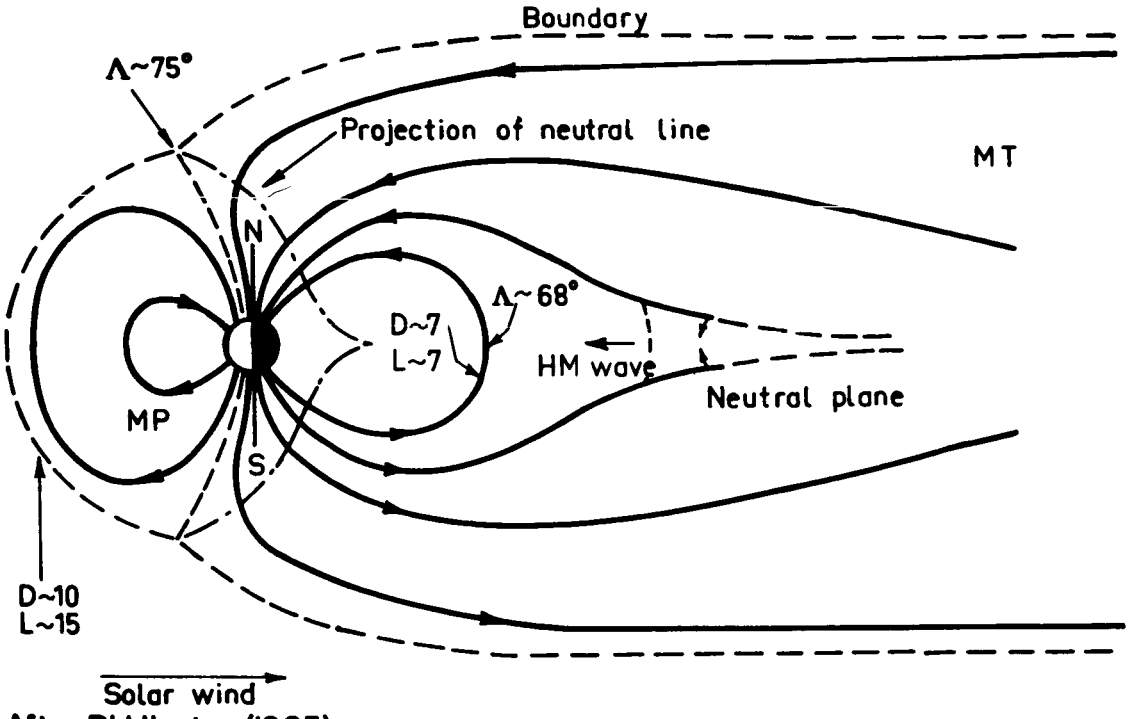

After Piddington (1965)

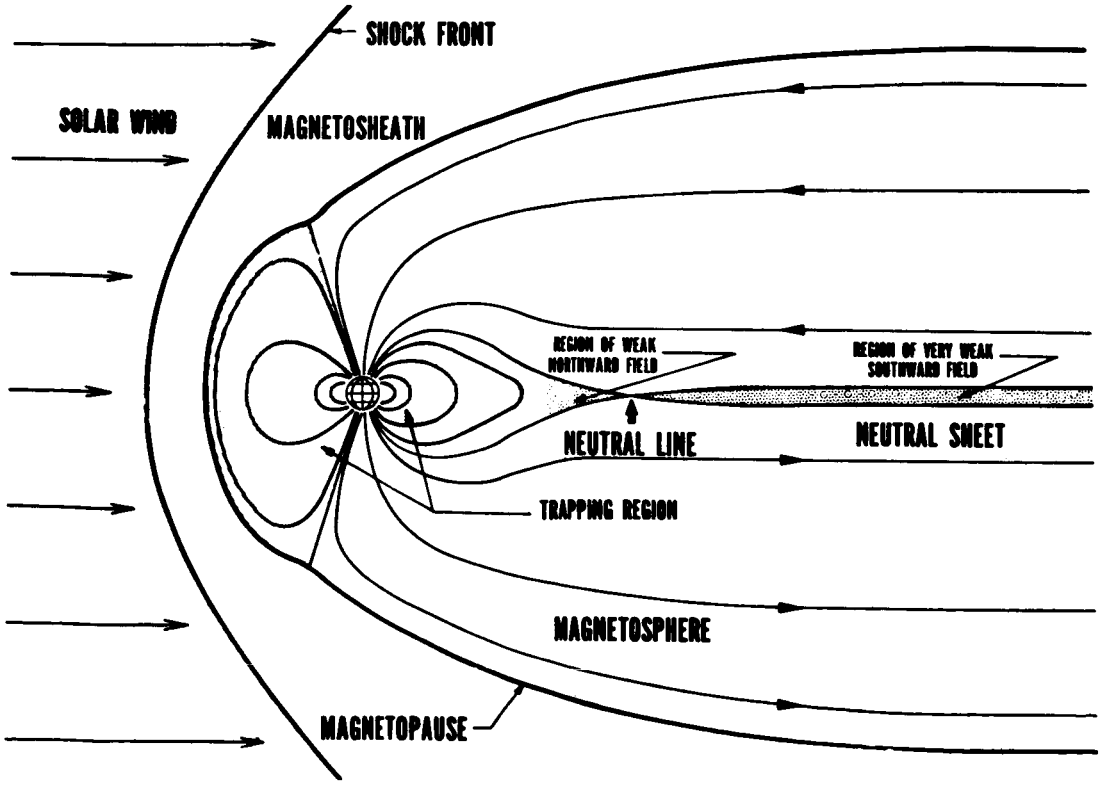

After Dessler (1968)

FIGURE 23